Order Number 9514185

# The Triton-Neptune plasma interaction

Hoogeveen, Gary William, Ph.D.

Rice University, 1994

U·M·I

300 N. Zeeb Rd.
Ann Arbor, MI 48106

RICE UNIVERSITY

# THE TRITON-NEPTUNE PLASMA INTERACTION

by

GARY W. HOOGEVEEN

A THESIS SUBMITTED
IN PARTIAL FULFILLMENT OF THE
REQUIREMENTS FOR THE DEGREE
DOCTOR OF PHILOSOPHY

APPROVED, THESIS COMMITTEE

Paul A. Cloutier
Professor of Space Physics and Astronomy
Director

John W. Freeman
Professor of Space Physics and Astronomy

Tamara S. Ledley
Senior Faculty Fellow
Space Physics and Astronomy Department

Peter J.A. Nordlander
Associate Professor of Physics

Houston, Texas
April, 1994

## ABSTRACT

The Triton-Neptune Plasma Interaction

by

Gary W. Hoogeveen

The Voyager 2 encounter with Neptune and Triton in August of 1989 provided clues to an intriguing problem. Instruments onboard the spacecraft showed a large ionosphere at Triton. Subsequent studies have tried to explain the production of such high levels of ionization but have ignored the possible plasma dynamics originating from the interaction between Neptune's magnetosphere and Triton. This study applies knowledge gained from studying the solar wind-Venus interaction to this case. In doing so we find that observations made by Voyager 2 can be explained by downward convection of magnetospheric plasma into Triton's atmosphere. Furthermore, we find that the flowing momentum is transferred to the moon just below the exobase, calculated here to be approximately 750 km. From this point down the atmosphere is not in hydrostatic equilibrium, and cannot be until below the ionization peak. Finally we show that when the momentum gets transferred to the moon the flow must shut off. This is accomplished when both the convective velocity and magnetic field go to zero. By showing the magnetic field vanishes at an altitude of roughly 650 km, we conclude the accepted mechanism by which the ionosphere is produced to be invalid. This mechanism was identified early-on to be impact ionization from hot, or superthermal, electrons originating in Neptune's magnetosphere. These precipitating hot electrons are thus shown to operate independently of the magnetic field below the exobase. This is a result not previously discovered, and one which implies that the plasma interaction between Neptune's magnetosphere and Triton cannot be ignored.

**Acknowledgements**

My most sincere appreciation is extended to my advisor, Dr. Paul Cloutier, for his generosity and wisdom throughout my graduate career. The numerous excursions to the Pioneer Venus Research Center South Annex were invaluable and much appreciated. I would also like to thank the rest of our group, which over the course of my stay at Rice consisted of Brian Stewart, Mark Matney, Leonard Kramer, Shannon Walker, and Colin Law. I would be terribly negligent if I failed to thank the people who operate this department and make it enjoyable on a daily basis: thank you Maria and Umbe.

However, my most heart-felt thanks go to my wife, Crystal. Her support during the past years could not be overstated. If she ever decides it is her turn to wade through her education, I hope to return the consideration and assistance she has so abundantly given to me.

This research was supported by NASA contract NAGW-3811.

## Table of Contents

## I. Introduction

Hot magnetized plasma flows interacting with planetary obstacles have been of fundamental interest since the solar wind was first predicted by Ludwig Biermann in 1951. Biermann noticed that the shape of cometary tails showed two very distinct streams emanating in the anti-sunward direction. One tail pointed directly anti-sunward, while the other tail simply was dispersed in the sun-orbital direction [*Dessler*, 1965]. Beirmann postulated that the tail pointing directly away from the sun "could only be accounted for by the radial flow of solar corpuscular fluxes." [*Parks*, 1991]. Eugene Parker and Joseph Chamberlain further studied this mysterious solar emanation, and argued about its characteristics. In the end, Parker's supersonic "solar wind" model proved accurate for the sun, while Chamberlain's subsonic "polar wind" was more pertinent to flows blown off from planetary atmospheres.

Nearly twenty years later, work began on computational solutions to supersonic gasdynamic flows related to rocket flights through Earth's atmosphere. From work done by *Spreiter et al.* [1970], supersonic gasdynamic flows were seen to be very similar to supersonic magnetohydrodynamic flows. Therefore, it is possible to group these MHD flows into certain categories for easier study, and as a result we can gain a better understanding through analogy.

In the simple gasdynamic fluid picture, a supersonic flow is diverted by a pressure wave propagating forward from the obstacle at the sound speed until it reaches the point where it is able to shock the flowing gas. This simple fluid picture is most analogous to our first space plasma-obstacle interaction: a planet with a completely neutral atmosphere. The problem with this analogy is that the solar wind's mean free path length is approximately 1 AU. This implies, in the ordinary fluid picture, that the solar wind

should not even see something as small as a planet. However, the solar wind is magnetized thereby causing it to interact on spatial scales equal to its gyro-radius instead of its collisional mean free path. The solar wind's gyro-radius, or Larmor radius, is

$$a_L = \frac{mV_\perp^2}{2eB}$$

For average solar wind conditions, V = 300 km/s and B = 10 nT, $a_L$ has a value of 300 km, a spatial scale much smaller than the radius of any planet. In this gasdynamic picture, the flowing solar wind would flow unimpeded to the point at which it collides with the neutral atmosphere of the planetary obstacle. This occurs at the exobase, defined to be the altitude where the mean free path of the flowing particles is equal to the scale height of the neutrals. Another way to state this is that the flow stops when it has passed through enough of the obstacle such that the probability of collision is high This gas is then able to transfer its momentum through collisional drag to the atmosphere, and then because the neutrals are gravitationally bound to the planet, to the planet itself. However, in magnetized plasmas the magnetic field also causes pressure gradients and carries momentum and hence, must be considered in the interaction.

Therefore, there exists a second form of interaction when the obstacle is magnetized. If the obstacle's magnetic pressure $\left(\frac{B_{ob}^2}{2\mu_0}\right)$ is greater than the flowing plasma total pressure

$$\rho v_{flow}^2 + (nkT)_{flow} + \frac{B_{flow}^2}{2\mu_0}$$

then the magnetic field is able to stand off the flow. It is important to note that in the solar wind there is a relationship between these pressures resulting from its flowing nature

$$\rho v_{flow}^2 >> (nkT)_{flow} > \frac{B_{flow}^2}{2\mu_0}$$

so that one needs only to compare the ram pressure with the obstacle's magnetic pressure. The manner in which the solar wind's momentum is then transferred to the obstacle is slightly different. In the simple gasdynamic picture the flowing momentum is transferred through collisional drag. However, in the case of plasma interactions with planets containing magnetic fields, the flow compresses the obstacle's magnetic field. This compression results in a non-zero local curl of B and therefore causes currents to flow at the interaction boundary. These currents are known as the Chapman-Ferraro currents and occur at the magnetopause. The resulting $\mathbf{J} \times \mathbf{B}$ force from this compression is transferred through the field to the interior of the planet, thereby transferring the momentum to the obstacle.

The final complexity in magnetized flow interactions results from adding an ionosphere to the obstacle. The ionosphere changes the dynamics of the solar wind by mass-loading it, and by allowing currents to set up inside it forcing the magnetic field to drape around the obstacle. Of course, if the magnetic field is substantial enough to stand off the flow outside the ionosphere, the complexity is reduced (e.g., the Earth). However, the interaction where the magnetic field is sufficiently small (or non-existent) and where there exists large neutral and ionized atmospheres is the most complex case, and consequently, most misunderstood. This is the situation at Venus.

During the first years of the Pioneer Venus mission there existed a debate concerning the solar wind interaction at Venus. One side held that the solar wind's Mach number changed continuously as it approached Venus proceeding smoothly through Mach one, and therefore there existed no shock but rather a very weak interaction [*Wallis*, 1973]. The opposite view held that the interaction consisted of the undisturbed solar wind encountering a strong shock in front of the planet [*Cloutier et al*, 1969]. The latter view held that Venus was mass-loading the solar wind to a much greater degree than the flow could handle without causing a sharp transition from supersonic flow to subsonic flow. Incidentally, the Mariner 2 mission in 1965 added fuel to this fiery debate. This spacecraft made two passes in front of Venus and found a strong shock in one case, and a weak shock the next. A little knowledge can be dangerous. Fortunately, the Pioneer Venus mission later showed conclusively that there did exist a very strong shock in front of Venus. The interaction is strong and in this manner, similar to the Earth's in which the magnetic field stands off the flow. However, Pioneer Venus also showed that Venus' magnetic field was certainly not strong enough to stand off the flow. In fact PVO could not even measure a magnetic field attributable to Venus [*Russell et al.*, 1979]. So how does the pressure get transferred from the solar wind to the planet in the case of a large ionized atmosphere with no intrinsic magnetic field?

Pressure transfer in a highly ionized but non-magnetized obstacle is very important. There are some who argue that the ionosphere is the mechanism by which the flow is stood off [e.g., *Phillips et al*, 1985; *Luhmann et al.*, 1984]. In their models they assert that the neutral atmosphere is important only when the flowing ram pressure exceeds the ionospheric thermal pressure. This model asserts that when the ram pressure equals the ionospheric pressure the flow stops. While in some ways this is true, the actual dynamics are much more complicated than that. In this view, one disregards the fact that the actual obstacle to the flow is the body itself. If the entire mass of the

ionosphere were set out alone in the solar wind, it would be caught up and blown back within a few gyro-periods. There simply isn't enough mass in Venus' ionosphere to stand off the flow. However, the planet itself is certainly massive enough. So how does this pressure get transferred from the solar wind through the ionosphere, the neutral atmosphere, and finally to the planet? The answer is a combination of transfer from ordered ram pressure through thermal pressure and magnetic field pressure, through atmospheric friction, and in the end, through gravitational weight.

## II. History of Flow/Field Model

In order to further understand the interaction with a non-magnetized body, one needs to study the role of the ionosphere. As alluded to previously, Cloutier and coworkers [*Cloutier and Daniell*, 1973; *Cloutier et al.*, 1974; *Cloutier*, 1976; *Daniell and Cloutier*, 1977; *Cloutier and Daniell*, 1979; *Cloutier et al.*, 1981, 1983; *Cloutier*, 1984] developed a steady state model resulting in the Venus flow/field model [*Cloutier et al.*, 1987]. It is a model of the flow velocity, density, and magnetic field from the ionopause to the exobase, including the exact details of the pressure transfer through the ionosphere. The information about the flow above the ionopause was obtained from Pioneer Venus data. This experimental data allowed the representation of the initial conditions at the top of the ionosphere, or the ionopause. With knowledge of the magnetic field, the various ion species' densities, and the ion and electron temperatures, Cloutier and coworkers were able to model the evolution of the flow down the ionosphere. They discovered they could accurately reproduce the observed ion density profiles as well as the magnetic field structure by solving the coupled equations of conservation of mass, momentum, and energy. They included various chemical reactions in their production and loss terms as well as the forces and heating supplied to the plasma as it flowed down the ionosphere. In order to reproduce everything as seen in the PVO data, they also had to assume additional heating in the ionosphere. Furthermore, this heat input had to increase with decreasing altitude. This necessity became interesting for a couple of reasons.

As work on the model continued, a related discovery was made. In analyzing PVO data, an unexplained and consistent deficit in pressure was seen as one descended in altitude from the unshocked solar wind down through the ionosphere [*Cloutier et al.*, 1993]. The total pressure must be conserved as one passes from the solar wind through the shock and into the ionosphere. Since the data showed that the total pressure measured

was not being conserved through this flow, there must be some sort of unmeasureed, or missing pressure that allows the total pressure to be constant along the flow line. This missing pressure displayed one very interesting characteristic: the absolute value of missing pressure began near 30% of the total solar wind pressure at the ionopause and monotonically decreased with decreasing altitude. This discovery was then utilized in the flow/field model. By incorporating this missing pressure profile the proper convergence of the model to the observed profiles from PVO occurred, without the previously required heat input.

Another interesting consequence of the previously monotonically increasing heat input, now replaced by the monotonically decreasing missing pressure, is the appearance of the "S" layer in the ionosphere of Venus. In certain situations, when there is a cooling in the plasma temperatures as the plasma descends in the ionosphere or when the missing pressure profile is steep enough, depending on which term is dominant, the vertical downward velocity will increase. In some situations the velocity can become comparable to the sonic velocity. This region always occurs just above the point at which the flow becomes heavily affected by collisions with the neutrals, i.e., the exobase. Above the exobase the flow is accelerated by the aforementioned reduction in pressures. It is entirely analogous to supersonic flow in a deLaval nozzle [*Landau and Lifshitz*, 1966]. As the walls in a deLaval nozzle are restricted in a subsonic flow, the flow speed increases. The increasing neutral collisions coupled with the subsequent cooling of the plasma acts as a constricting nozzle and drives the flow downward. This phenomenon has been independently modeled in simulations of in-falling material around galaxies where the flow behavior is known as "cooling flow" [*Fabian*, 1988]. Furthermore, in an area more easily associated with the interaction at Venus, researchers have recently independently discovered this acceleration of flow in Mars' planetopause [*Sauer et al.*, 1991]. As a side note, they designated this layer as the "T" layer, representing the

transition from subsonic to possibly supersonic flow. The "T" layer was actually the first choice in the 1987 Cloutier et al. paper, however, it was decided that "T" wasn't as physically meaningful as "S" [personal communication].

The flow/field model showed that by allowing a small amount of solar wind into the obstacle, with the vast majority of it simply flowing around, the conditions reported by PVO could be reproduced. However, there still remained this uncertainty concerning the role of the ionosphere. Just how important was it in the interaction? To address this issue, we asked the question, "What would happen if a supersonic flow encountered a planetary body with no intrinsic photochemical ionosphere?" This question was actually posed much earlier by *Michel* [1971]. The answer came in work done by *Hoogeveen* [1992] in which he modeled a situation where a magnetized plasma encountered a moon-sized obstacle, with a significant neutral atmosphere, but no solar-induced ionosphere. The motivation for these conditions will become apparent later. In brief, for the steady-state equations to be satisfied for these conditions, the incoming flow had to be 2-3% of the incident flow, and had to be subsonic [*Hoogeveen*, 1992]. These requirements are satisfied at Venus, indicating that even without an intrinsic photochemical ionosphere there must be an interaction with Venus. Furthermore, the Hoogeveen study showed conclusively that the pressure in the supersonic flow is easily transferred through the atmosphere to the planet, as long as the atmosphere is magnetized down to the exobase. Therefore the argument that the ionosphere is necessary to transfer the solar wind momentum to Venus is refuted.

This theoretical study of a neutral-only atmosphere interacting with a flowing plasma was necessary to show that if the conditions are right, there must be an interaction. But is there actually any situation in the universe that satisfies these conditions? The motivation for using parameters similar to a moon orbiting a large planet now becomes evident. By using parameters similar to those of Triton, a moon

orbiting Neptune, the next step in reality was easily taken. Through the closer study of the chemistry in Triton's ionosphere, we were able to change this hypothetical planetary body in Hoogeveen's study to a real-world obstacle.

## III. Triton

Triton represents a fascinating case study in plasma flows and interactions. Voyager 2 completed a flyby with Neptune's system in August of 1989 (see figure 1). The instruments onboard the spacecraft provided information concerning Neptune's magnetic field, the composition of the magnetosphere, the mass of Triton, the atmospheric composition of Triton, the existence of a strong ionosphere at Triton, and the geometry between Neptune and Triton (see figure 2). It was confirmed that Triton is in a retrograde orbit with an effective velocity difference between the corotational magnetosphere and itself of 42.9 km/sec. This information allowed for a realistic model of the interaction between Triton and Neptune's corotational magnetosphere. Before describing our model in more detail or analyzing the other models attempting to explain the Voyager 2 results, we shall take a closer look at the instruments onboard Voyager 2 and their findings.

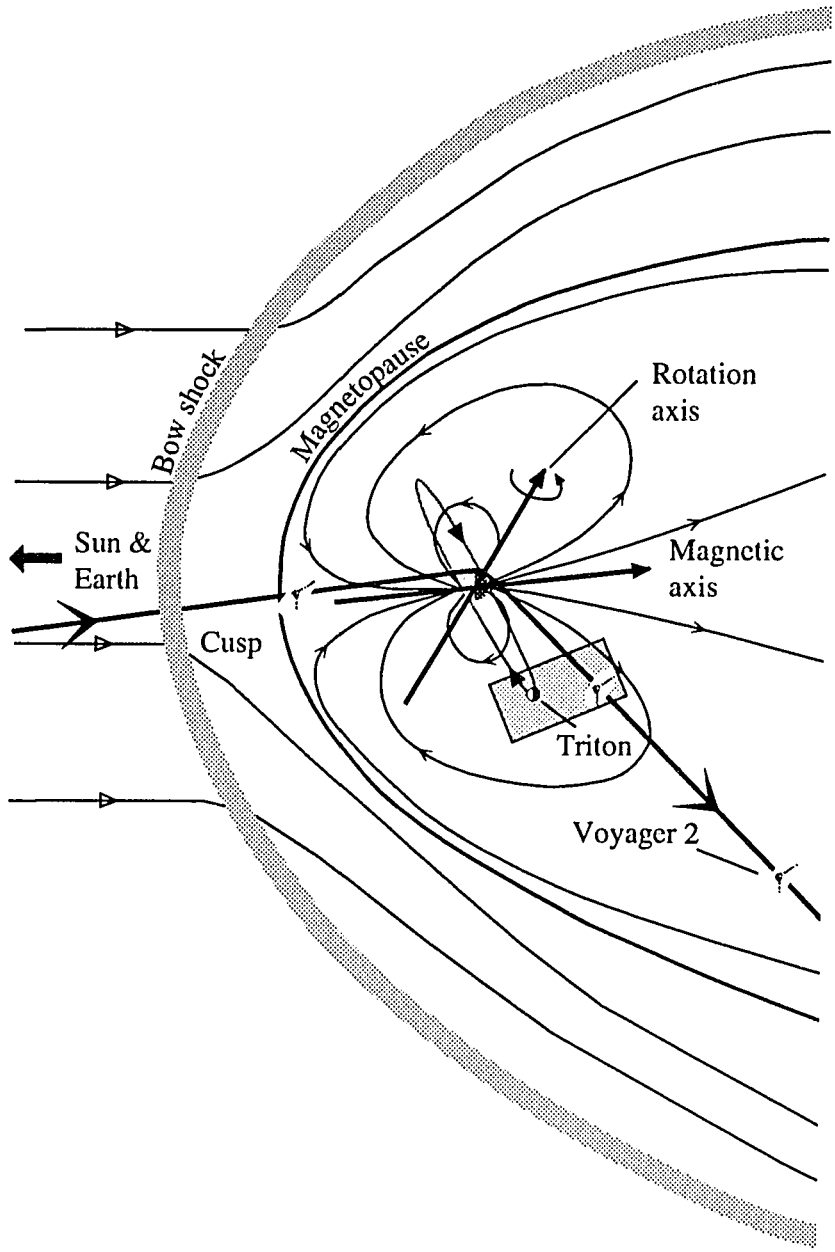


Figure 1. A sketch of the Neptune system in the noon-midnight meridian plane, [after *Belcher et al.*, 1989]. Notice the highlighted rectangle around the vicinity of Triton. Figure 2 is a blowup of this area.

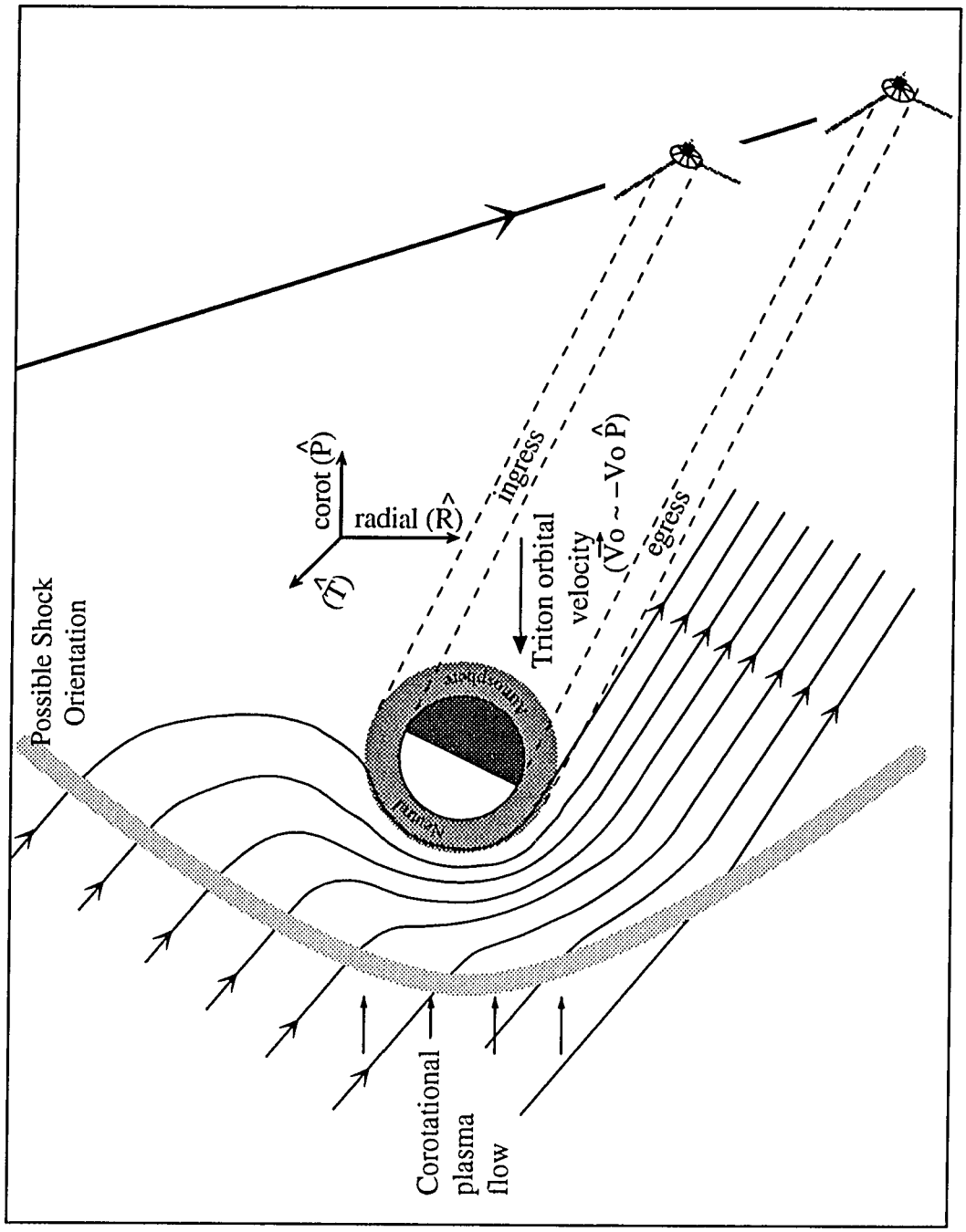


Figure 2. An enlargement of the vicinity around Triton. Neptune is towards the top of the page, in the minus radial direction. The corotational flow impinges from the left with velocity, $V_0$, relative to Triton. The shock is only representative of the fact that the flow must be subsonic as it enters the atmosphere; the actual shock may be Alfvén Wing mode.

## III.A. Voyager 2 at Neptune and Triton

The Ultraviolet Spectrometer Experiment (UVS) onboard Voyager 2 used during occultation on August 25, 1989, discovered that Triton possessed a substantial neutral atmosphere. In figure 3 we see that for a model with a temperature of 95 K above 400 km altitude, the data is well represented by assuming the neutral species is molecular nitrogen. Furthermore, the model reported by the UVS team [*Broadfoot et al.*, 1989] assumes a deposition of heat at 400 km to reproduce the isothermal atmosphere above 400 km. The surface column density of $N_2$ is $3.8 \times 10^{21}$ $cm^{-2}$, which is equivalent to the amount of Earth's atmosphere above the altitude of 65 km. The team also reported densities and temperatures for a methane component in the lower atmosphere. Subsequent studies have used the knowledge of methane densities to calculate possible chemical interactions resulting in large quantities of atomic nitrogen as well as molecular and atomic hydrogen. These later studies will be discussed in more detail in the following sections.

Voyager 2 also carried a Radio Science experiment (RSS). During the previously mentioned occultation of August 1989, the RSS observed a sizable ionosphere. *Tyler et al.* [1989] report peak electron densities of $2.2 \times 10^4$ $cm^{-3}$ at ingress, and $4.7 \times 10^4$ $cm^{-3}$ at egress (figure 4). These values are comparable to electron densities found in the D region of the Earth's ionosphere. These relatively high densities are quite surprising, for many reasons. Data taken during the Saturn encounter by Voyager 1 showed little or no ionosphere on Titan. *Tyler et al.* [1981] show that the peak electron density at Titan was only $3 \times 10^3$ $cm^{-3}$, roughly an order of magnitude smaller than Triton's. Even though Titan is considerably larger than Triton, and the fact that Titan is 9.5 AU from the sun while Triton is 30.2 AU away, Triton shows a much larger ionosphere. If the sole factor

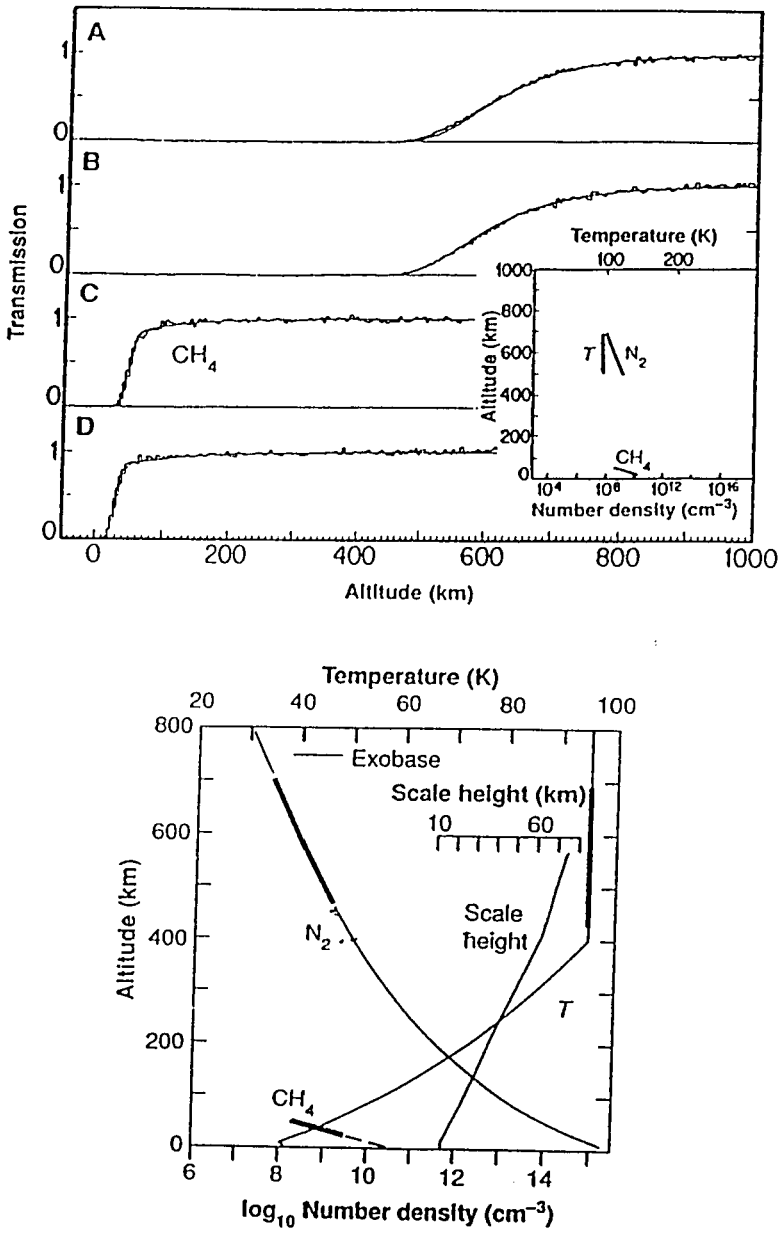


Figure 3. Triton solar occultation. (A and B in top panel) Ingress and egress light curves at short wavelengths, where extinction is due to the $N_2$ ionization continuum. The solid lines show the transmission calculated from models with a temperature of 95 K above 400 km. (C and D in top panel) The inset in the top graph shows measured number densities and temperatures. The bottom panel shows the model neutral atmosphere. Both graphs taken from *Broadfoot et al.*, 1989.

for generating the ionospheres of both Titan and Triton were solar EUV, the density at Titan should have been more than ten times Triton's, due to the $r^{-2}$ factor. However, this was not the case.

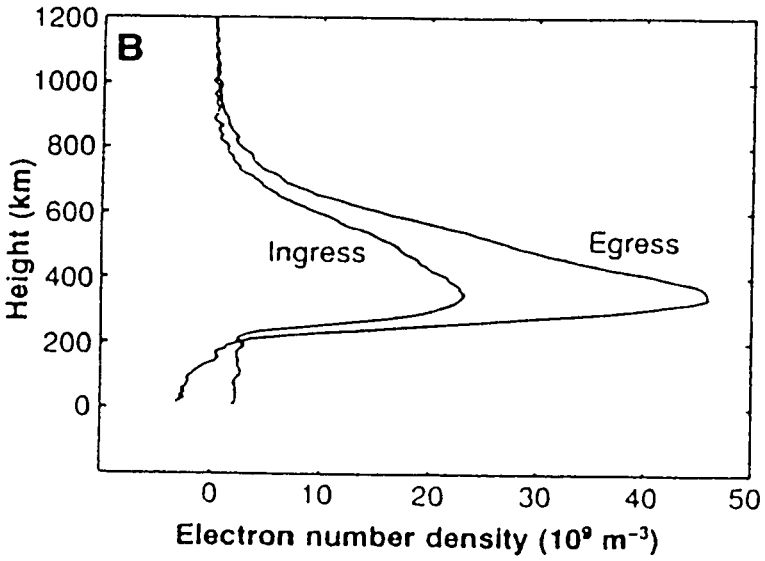


Figure 4. Electron number density profiles obtained from inversion of observed phase profiles. The peak electron densities are reached at about the same height (~340 to 350 km). From *Tyler et al.*, 1989.

This leads to the assumption that there must be an interesting and strong interaction between Triton and Neptune's magnetosphere. Somehow Neptune's magnetosphere is substantially ionizing Triton's atmosphere in a way that Saturn's magnetosphere does not affect Titan. We postulate that the interaction is stronger because Triton moves supersonically in Neptune's magnetosphere, while Titan is subsonic in Saturn's. Thus the interaction more closely resembles the Venus-solar wind interaction than does Titan. Although Titan exhibits many similarities to this type of interaction, the fact that it is never supersonic inhibits a strong interaction.

The magnetometer onboard Voyager 2 was used to measure the ambient magnetic field in Neptune's magnetosphere. The spacecraft's closest approach to Triton was

approximately 23.4 $R_{eff}$ [*Neubauer et al.*, 1991], where $R_{eff}$ is defined to be the radius of Triton plus the altitude at which the ionospheric density peaks, i.e.,

$$R_{eff} = R_T + R_{ionopeak} = 1352 \text{ km} + 345 \text{ km} \approx 1700 \text{ km}$$

At 23.4 $R_{eff}$, magnetometer data show a stable magnetospheric field from Neptune but no signature attributable to Triton [*Ness et al.*, 1989]. For all intents and purposes, Triton can be considered to be non-magnetized, thus demonstrating that in this area the interaction between Venus and the solar wind is similar in nature to the Triton-Neptune interaction.

Before a complete description of the interaction is possible, we need information about the corotating plasma. Voyager 2 observed two distinctly different populations of magnetospheric plasmas. The plasma instrument reported what we designate as the thermal component, and the Low Energy Charged Particle (LECP) experiment discovered a hot, or superthermal, component. For the inbound plasma sheet crossing [*Belcher et al.*, 1989], the $H^+$ thermal density and temperature were $n_p$ = 0.07 cm-3 and $T_p$ = 7 eV, respectively, and the $N^+$ thermal density and temperature were $n_{N^+}$ = 0.04 cm-3 and $T_{N^+}$ = 65 eV. The superthermal population, most recently reported by *Mauk et al.* [1994], shows an electron density of $10^{-3}$ $cm^{-3}$ at a temperature of roughly 20 keV. This corresponds to a superthermal pressure of nearly 3 x $10^{-12}$ N $m^{-2}$.

The thermal sound speed in the plasma sheet is given by

$$C_s = \sqrt{\frac{\gamma p}{\rho}}$$

where p and $\rho$ are total pressure and density, and $\gamma = 2$ for a magnetized plasma. If $T_{eth}$ = 30 eV [*Strobel et al.*, 1990a], $C_s$ is then approximately 44 km/s. Using the same plasma parameters and a magnetic field of 8 nT [*Ness et al.*, 1989], the Alfvén speed

$$C_A = \sqrt{\frac{B^2}{\mu_0 \rho}}$$

is 220 km/s. Triton's orbital velocity is - 4.4 km/s and the corotating plasma at 14 $R_N$ has a velocity of 38.6 km/s [*Strobel et al.*, 1990a]; Triton's synodic velocity ($V_N$ - $V_T$) is 43 km/s. Thus Triton's sonic Mach number $M_s$ is $\approx$ 1, but its Alfvén Mach number is very much less than one ($M_A \leq 0.2$).

According to *Neubauer* [1990] this regime of plasma parameters indicates that there should not exist a bow shock in front of Triton. In the case where $M_A < 1$ and $Ms \geq 1$, the standard disturbance system consists of Alfvén wings and slow disturbances of variable strength. All of this is of no great significance as it pertains to this study. The exact method by which the plasma is slowed from supersonic to subsonic velocities is not important. What we know must happen, as will be discussed later, is that the flow must be subsonic at the ionopause. This is the only stipulation made on the incident flow. Therefore the fact that the Venus-solar wind interaction has a strong bow shock, but Triton does not, is unimportant. What is important is that the flow is mostly diverted, with only a small fraction entering the top of the ionosphere and driving the dynamics of the interaction.

### III.B. Previous Studies

Since the 1989 Voyager 2 flyby, a number of researchers have attempted to model Triton's ionosphere and neutral atmosphere. For the most part these studies have used known atmospheric chemistry to expand the first-look models to include atomic nitrogen as well as molecular and atomic hydrogen. By incorporating these reactions, they hoped to describe the aeronomical processes taking place in Triton's atmosphere more accurately. However, many studies assumed chemical and hydrostatic equilibrium and ignored any possible dynamics from the flowing magnetospheric plasma. They all assumed that magnetospheric electrons were precipitating down field lines into Triton's atmosphere, but failed to include the requisite magnetic field effects. A closer examination of each study found in the literature is helpful.

As reported by *Broadfoot et al.* [1989], the model of the neutral atmosphere which best fits the data requires an atmospheric heating flux of 0.0016 erg $cm^{-2}$ $s^{-1}$. Precipitating particles from Neptune's magnetosphere were identified as a possible ionization and heating source by *Tyler et al.* [1989]. Taking the lead from these reports, investigators such as *Yung and Lyons* [1990], *Ip* [1990], *Strobel et al.* [1990a], *Strobel et al.* [1990b], *Summers and Strobel* [1991], *Majeed et al.* [1990], *Lyons et al.* [1992], *Stevens et al.* [1992], and *Krasnopolsky et al.* [1993] developed independent models describing the interaction. Each model assumes different conditions such as neutral concentrations and scale heights, ion and neutral chemistry, and methods of ionization and atmospheric heating. A brief description of the models follows:

a) *Strobel et al.* [1990a,b], *Majeed et al.* [1990], and *Summers and Strobel* [1991]: These four studies model the neutral atmosphere as eddy diffusion dominant up to a homopause ranging from 135 km to 300 km. As a result of efficient atmospheric mixing

and methane photolysis in the lower atmosphere, high levels of H and $H_2$ are present throughout the atmosphere extending past 1000 km. These studies employ additional production and heating from a Chapman-like electron precipitation mechanism. Each model identifies $N^+$ as the major ion above the ionization peak, and a combination of $N^+$, $N_2^+$, and $H^+$ below the peak (figure 5). They assume photochemical equilibrium and ignore any dynamics resulting from the interaction between the magnetospheric plasma and Triton's atmosphere. *Strobel et al.* [1990a] evaluate the possibility of two types of entry for the energetic particles, and conclude that curvature drift into the ionosphere dominates over direct convection due to high ionospheric Pederson conductivity.

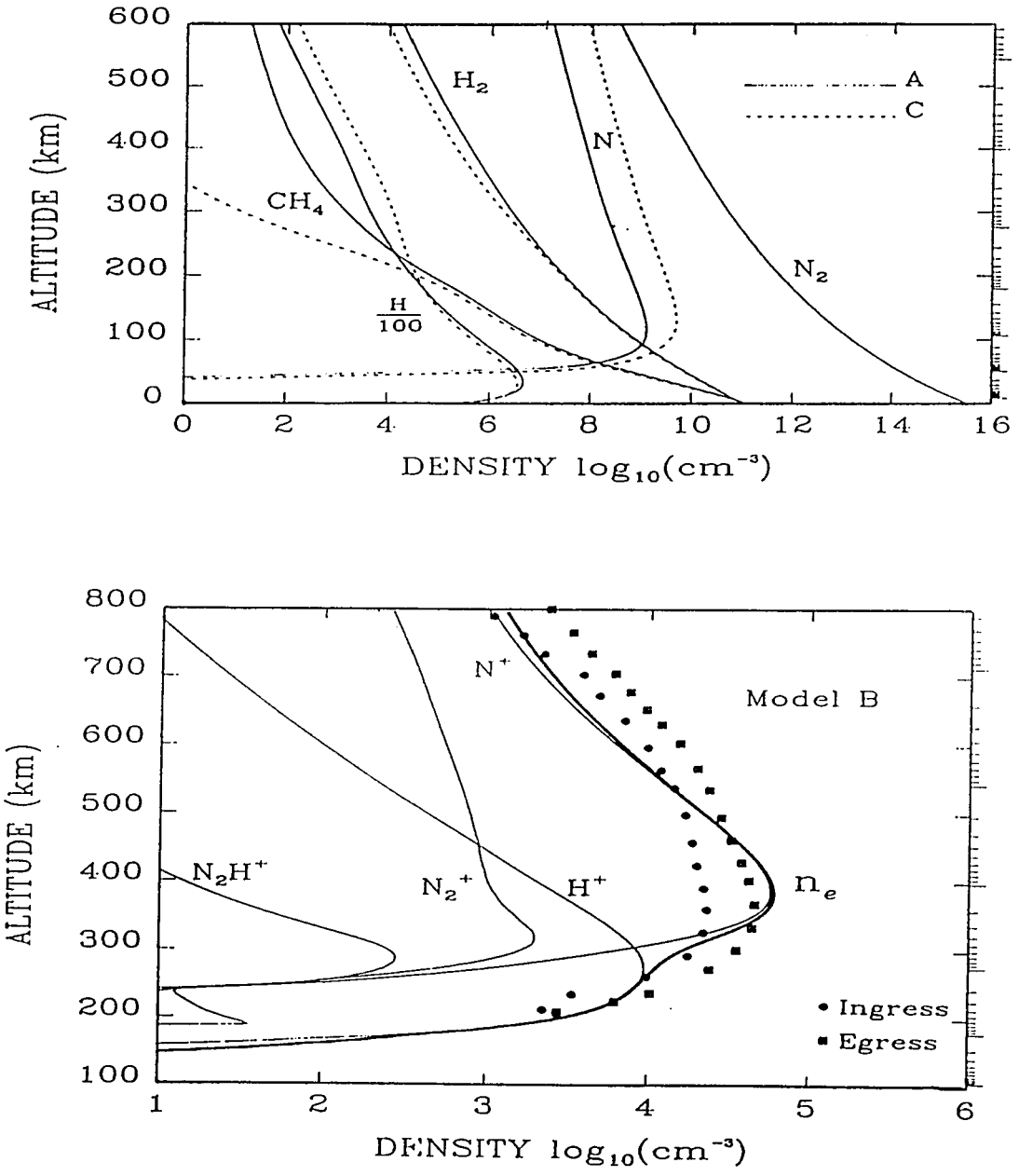


Figure 5. Top panel shows the modeled neutral atmosphere. The solid lines, labeled A, are the results of the more favorable run. The bottom panel compares the calculated ion densities with the observed electron density reported by *Tyler et al.*, 1989. Both panels are taken from *Summers and Strobel*, 1991.

b) *Yung and Lyons* [1990]:

This study solves the coupled continuity equations for ions and electrons with transport by ambipolar diffusion. They show that a pure $N_2$ atmosphere requires too much heat influx from Neptune's magnetosphere to satisfy the neutral atmospheric model by *Broadfoot et al.* [1989]. They postulate $N^+$ to be the major ion throughout the ionosphere produced mostly by magnetospheric precipitation (figure 6). The inclusion of ambipolar diffusion attempts to explain the fact that the plasma scale height is not twice the neutral scale height, as is expected in a photochemical equilibrium situation, but, rather, is less than twice the neutral scale height. However, they conclude that they cannot completely explain the interaction since the atmospheric heating due to the required electron precipitation is still five times what is allowed by *Broadfoot et al.* [1989].

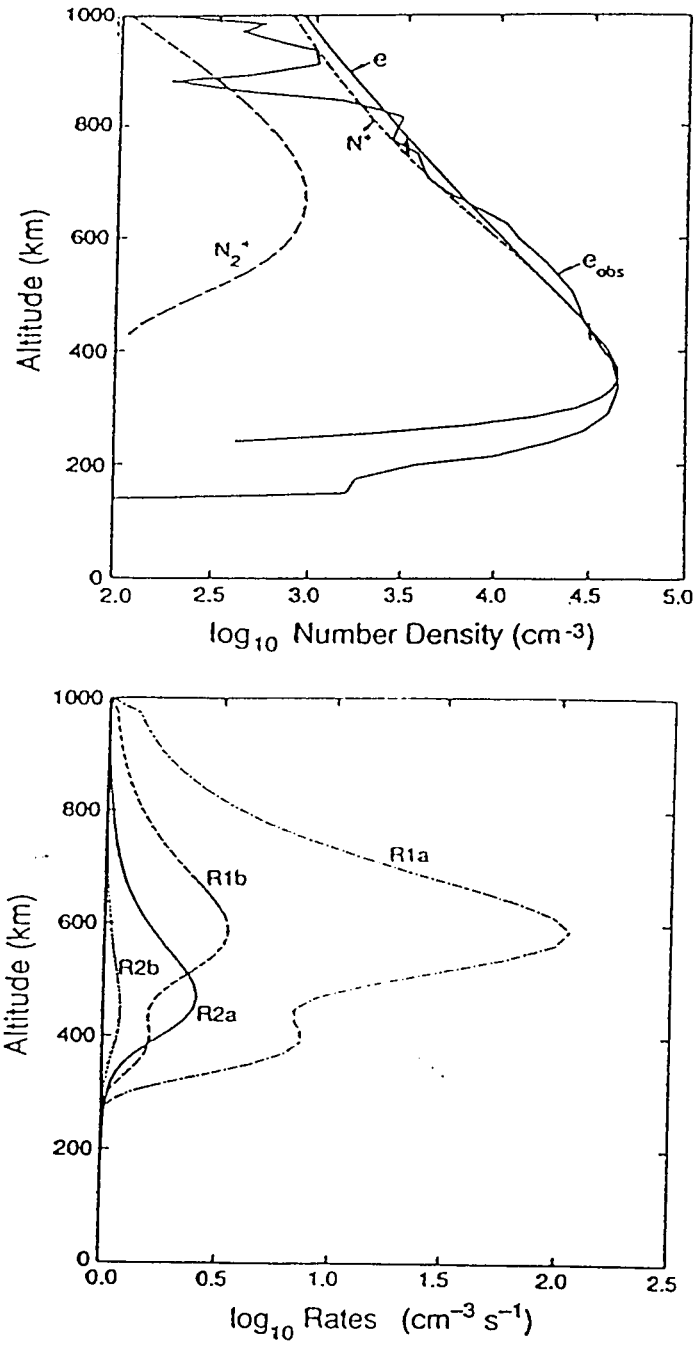


Figure 6. Top panel compares modeled ion densities to observed electron densities. Note that $N^+$ dominates throughout the topside ionosphere. Bottom panel shows ionization rates of N2+ (R1a) and $N^+$ (R1b) by electron impact, and photoionization rates for $N_2^+$ (R2a) and $N^+$ (R2b) in the model. Taken from *Yung and Lyons*, 1990.

c) *Ip* [1990] and *Hartle et al.* [1982]:

Ip's study concentrates on the mechanism of magnetospheric electron precipitation into Triton's atmosphere. He references the *Hartle et al.* work at Titan as a possible model for the precipitating electrons. Ip describes electrons bouncing along Neptune's magnetic field lines and curvature drifting into Triton's atmosphere. He calculates expected ionization rates and resultant electron density profiles (figure 7). Ip identifies electrons in the range of 10-20 keV as the population of precipitating magnetospheric electrons responsible for producing $N^+$, which he identifies as the major ionospheric constituent. However, in order to reproduce the electron density peak at 350 km, a much higher precipitating electron energy is required. These studies mention the necessary existence of significant magnetic fields down to altitudes of 200 km in order to allow electron precipitation at levels needed to reproduce observed electron densities.

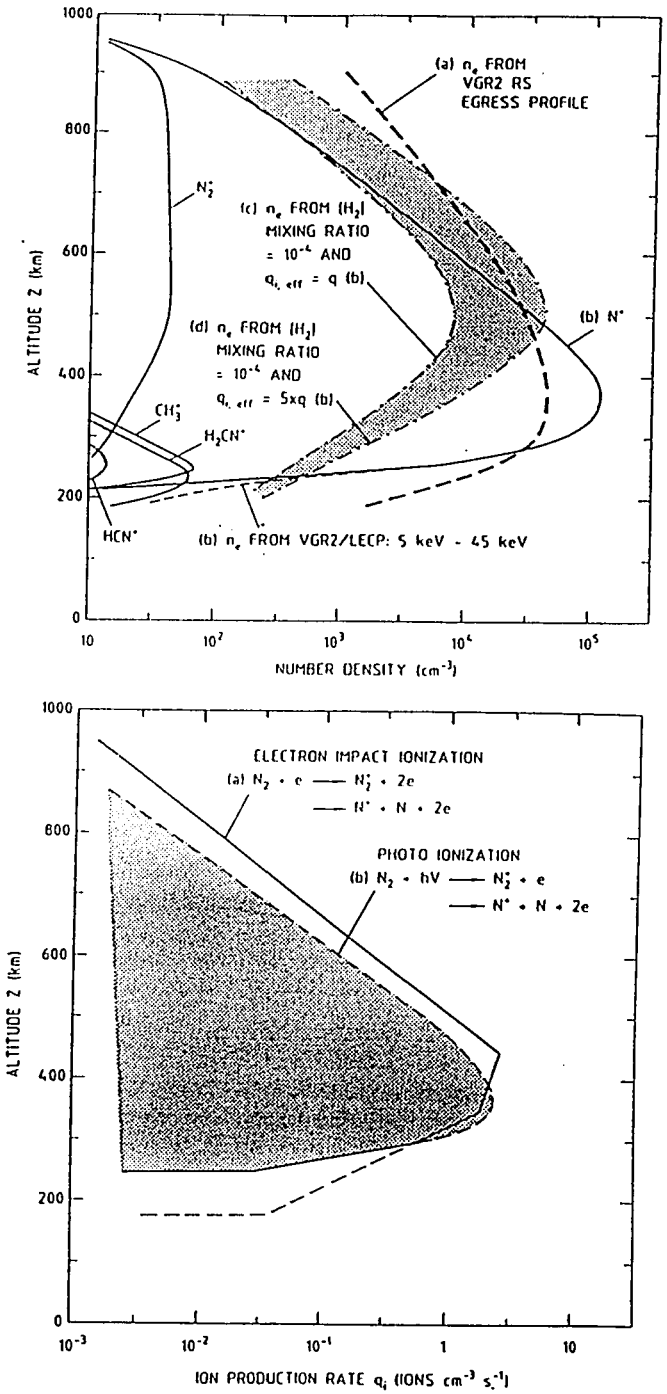


Figure 7. Top panel reports ion number densities. Bottom panel indicates ionization rates for both impact ionizations and photoionizations. Ip's model for impact ionization is seen to be considerably smaller than Yung and Lyon's reported in figure 6. From *Ip*, 1990.

d) *Lyons et al.* [1992]:

In this model an attempt was made to find an ionosphere which would not be controlled by Neptune's magnetosphere, but could rather be produced exclusively by solar EUV. They discovered that by incorporating carbon into the atmospheric chemistry they were able to reproduce the electron density profiles with reasonable assumptions of unknown chemical rates. Over 190 reactions and 39 neutral and ion species were included in a comprehensive one-dimensional photochemical model of Triton's atmosphere and ionosphere. They identified $C^+$ as the dominant ion throughout the ionosphere (figure 8). Even though they showed that electron precipitation is not needed, they admit that it probably does contribute in some way since EUV heating is too small by a factor of two to account for an isothermal thermospheric temperature of 95 K.

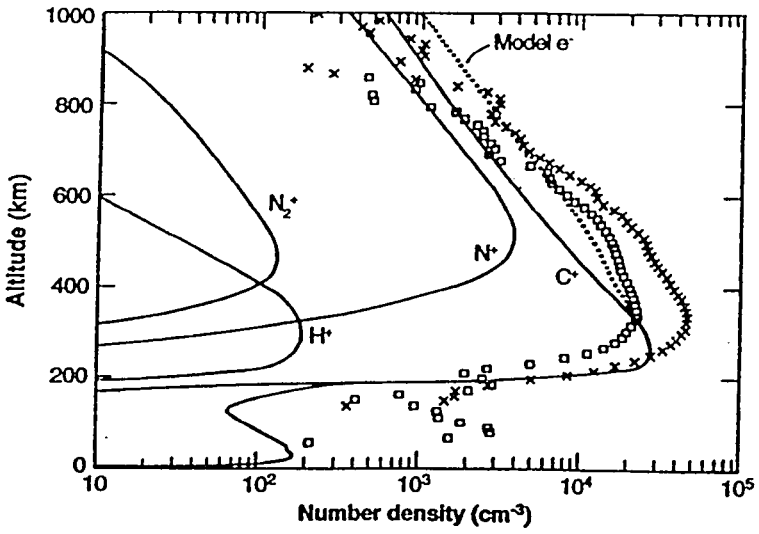


Figure 8. Ion and electron densities. The measured electron density profile for Triton's summer and winter hemispheres are taken from *Tyler et al.* [1989]. The squares and crosses are data from ingress and egress observations, respectively. From *Lyons et al.*, 1992.

e) *Krasnopolsky et al.* [1993]:

This is perhaps the most comprehensive study done on Triton's neutral atmosphere. Compared to the *Stevens et al.* [1992] paper, Krasnopolsky et al. have included more chemistry and have been more tightly constrained by the results from the UVS experiment. In their paper, Krasnopolsky et al. site certain insufficiencies in the *Stevens et al.* [1992] paper and correct them. In the end, this study finds a slightly different model than the original model used by *Broadfoot et al.* [1989] which, they feel, better fits the raw data. The new neutral model has an isothermal temperature of 104 K, instead of the previous 95 K, down to roughly 400 km. Below this altitude, the temperature assumes a lapse rate such that the surface temperature equals 38 K. They also calculate different nitrogen densities throughout the atmosphere, resulting from further analysis of a distinct step-like absorption feature at 850 Å in the UVS results [*Krasnopolsky et al.*, 1993]. This study claims this feature is due to the ionization of atomic nitrogen, and thereby calculates a more accurate neutral atmosphere population. The neutral species' profiles are shown below (figure 9).

With the exception of the Krasnopolsky et al. study, which did not attempt to model the ionosphere, each study detailed above failed to completely model the interaction. In the cases of assumed photochemical equilibrium, MHD dynamics were ignored. In the studies that mentioned dynamics (e.g., *Yung and Lyons* [1989]), they did not include magnetic field effects, nor did they satisfy the heating requirement set forth by *Broadfoot et al.* [1989]. For those instances where magnetic fields were included to model the precipitating electrons, adequate flow considerations were not made. And in the one paper that discussed the magnetospheric interaction [*Strobel et al.* 1990a] direct convective flow into the atmosphere was disregarded even though we know it plays an important role in the interaction at Venus [*Cloutier et al.*, 1987].

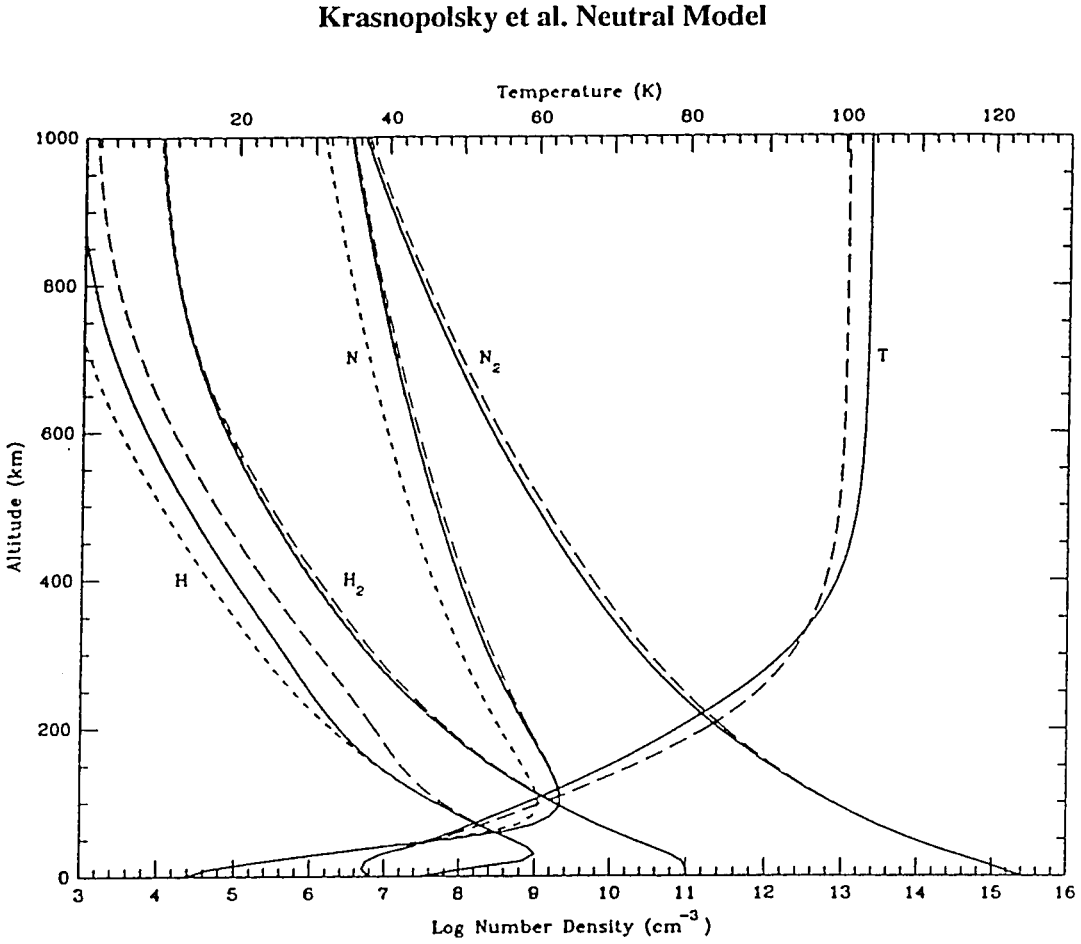


Figure 9. Temperature and $N_2$, N, $H_2$, and H density profiles of Triton's atmosphere. The solid lines represent the model which best fit the data. Taken from *Krasnopolsky et al.*, 1993.

## IV. Motivation for Flow/Field

In reviewing the aforementioned published studies it is evident that they are incomplete. Each case attempting to reproduce the ionospheric profile found it needed an extra production mechanism. This mechanism was invariably identified as impact ionization from precipitating electrons originating from Neptune's corotational magnetosphere. However, each study proposing this mechanism ignored all dynamics associated with the actual interaction between the corotational plasma, consisting partly of these hot electrons, and Triton's atmosphere. They assumed these hot electrons were producing ions in Triton's ionosphere, but they neither modeled other effects, such as heating of the plasma, nor considered how they arrived in Triton's atmosphere.

One study, [*Ip*, 1991] did attempt to explain the mechanism by which the hot magnetospheric electrons produce the ions in Triton's ionosphere. However, even this study, which referenced a study performed for Titan [*Hartle et al.*, 1981], stopped short of actually including the interaction dynamics. As explained previously, Ip required the magnetic field, which necessarily must be Neptune's since Triton is non-magnetized, to exist to altitudes as low as 200 km. Ip then went on to model the entire ionosphere as unmagnetized, thereby ignoring any dynamics associated with the interaction which causes the magnetospheric electrons to arrive at Triton in the first place.

Another study, [*Strobel et al.*, 1990], reinforces the assumption that Triton's ionosphere is unmagnetized. This study also concludes that there must be additional ionization in the ionosphere, most likely originating from hot electrons precipitating along field lines into Triton's ionosphere. They invoke the precipitation mechanism to explain one thing but then ignore its effects everywhere else.

Our study realizes these assumptions are contradictory and attempts to model the entire interaction self-consistently. Previous studies simply attempted to reproduce ionospheric profiles through photochemical equilibrium models, found that approach failed and then incorporated an additional ionization source. This study, however, attempts to reproduce the ionosphere through an analysis of the total plasma dynamics resulting from the interaction. We do not assume the ionosphere is unmagnetized, as do all other studies. Furthermore, we assume that the precipitating electrons are not simply a production mechanism. In this study it is recognized that a superthermal population as large as is required to populate the ionosphere also must carry a significant amount of momentum and energy. We incorporate the hot electron's pressure into our analysis, and show it transferring to the atmosphere simultaneously with the rest of the plasma's pressures. Finally, we consistently model the energy transfer from the flowing hot population to the cold ionospheric plasma. Previous studies ignored the heating that occurs when superthermal electrons collide with cold neutrals; we model this heating and show that it is very important in the overall transfer of momentum and energy from the flowing plasma to the obstacle.

The discrepancy over the extra production mechanism was not the only motivating factor for this study. The data from the Voyager 2 spacecraft revealed an interesting fact about Triton's atmosphere. As can be seen from figures 3 and 4, the scale heights of the plasma and neutrals have the following characteristic

$$2H_n > H_i > H_n$$

Numerically, the scale heights were reported to be

$H_n = 85 \pm 5$ km [*Broadfoot et al.*, 1989]

$H_i = 128 \pm 25$ km [*Tyler et al.*, 1989]

For an ionosphere in photochemical equilibrium the ion scale height should equal twice the neutral scale height. Thus it is obvious that the studies that simply solve the equations of photochemical equilibrium are necessarily flawed; the ionosphere cannot be in photochemical equilibrium.

Not all studies assumed photochemical equilibrium, however. Some researchers realized the aforementioned discrepancy [*Yung and Lyons*, 1990; *Summers and Strobel*, 1991] and tried to rectify it by invoking ion escape. They argued that in order to suppress the top-side ion scale height (i.e., increase $H_i$ in order to match $2H_n$), there must be additional losses in the top-side ionosphere. With the proper ion loss rate, which they attributed to unspecified mechanisms forcing ions to escape out the top of the ionosphere, the scale height relationship could realistically be explained in their models.

An alternate explanation for the suppression of the top-side ion scale height is downward convection. In studies performed at Venus and Mars, Cloutier and coworkers have shown that downward convection resulting from the solar wind-ionosphere interaction is equivalent to a loss mechanism and thereby suppresses the top-side ionosphere [e.g., *Cloutier et al.*, 1969; *Cloutier et al.*, 1987]. Therefore this study postulates that the top-side ionospheric profile at Triton can be explained without invoking the additional mechanism of ion escape. It is simpler to assume that the mechanism which is producing the extra ionization lower in the atmosphere is the same one which is removing it from higher altitudes. In the flow/field model, we model the suppression of the top-side ion scale height resulting from downward flowing plasma due to the interaction with Neptune's corotating magnetosphere.

In short, this study is motivated by a number of interesting characteristics that either have been addressed improperly, or not addressed at all. First, the mechanism by which the ionosphere is populated requires the existence of a magnetic field, yet no one has included it in any previous models. Second, the suppression of the top-side ion scale height demands that the ionosphere is not in photochemical equilibrium, a fact many studies have not recognized. Furthermore, the scale height anomaly has a different possible explanation than previously published studies have given: downward convection. Finally, downward convection does not conjure up an additional unknown mechanism to explain the suppression of the scale height. Rather it is a straight forward result of the mechanism by which the ionosphere is produced. That is, this study assumes one less unknown phenomena than other studies to explain all the observed characteristics recorded by Voyager 2.

For these reasons it is important to look closer at the flow/field model. By understanding its assumptions and details one is more able to come to the conclusion that previous models have not been sufficiently thorough. The next chapter gives explicit details behind the flow/field model and attempts to take the reader through each step in the formal solution of the problem.

## V. Explanation of Flow/Field Model

As stated previously, the details of the shock and interaction above the ionopause are secondary in this study. All that is required by the obstacle is to affect the initially supersonic flow in such a way that it is subsonic once it enters the atmosphere. Furthermore, the configuration of the magnetic field must be changed such that it is horizontal to the obstacle. These two criteria are satisfied at Venus through the appearance of a fast mode bow shock, however, this is not a strict requirement. In this case, the interaction is most likely through Alfvén wing disturbances [*Neubauer*, 1990]. Regardless, we have the same initial conditions at the tops of both atmospheres at Venus and Triton, thereby allowing a similar treatment in modeling.

One glaring difference, however, between Venus and Triton is their relative size. Venus' radius is 6053 km while Triton's is only 1352 km. This difference needs to be considered in modeling the interaction for two reasons. First, due to Triton's small size its gravitational field is significantly different at the top of the atmosphere, here considered to be 1000 km, then at the bottom. The difference

$$\%\Delta g = \left| \frac{\frac{1}{r_B^2} - \frac{1}{r_T^2}}{\frac{1}{r_B^2}} \right| = \left| 1 - \frac{r_B^2}{r_T^2} \right| \approx 60\%$$

is significant. As a result, the scale heights and the gravitational forces on the plasma needed to be calculated in the Triton model at every altitude as opposed to the model at Venus, where they were not . Figure 10 shows just how greatly the gravitational acceleration changes with altitude.

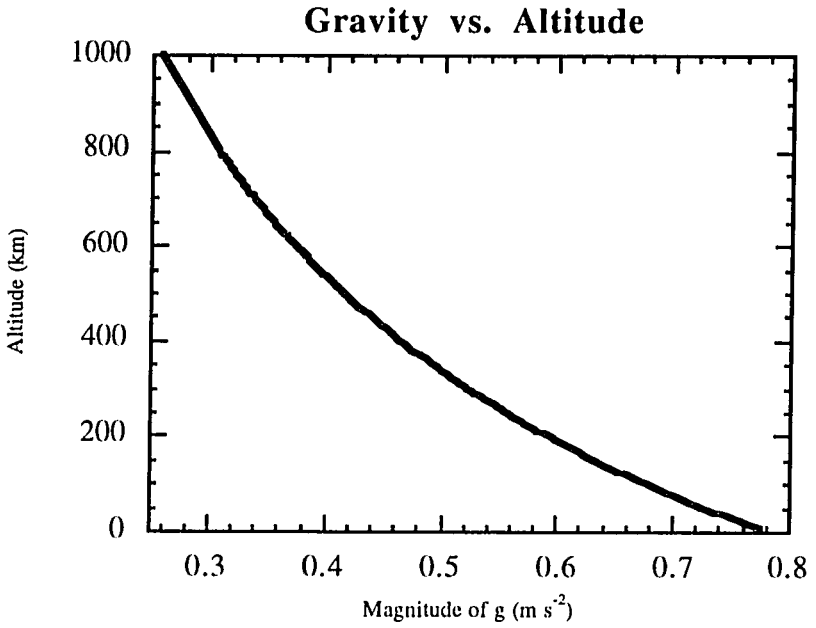


Figure 10. Plot of gravity versus altitude. Notice due to Triton's small radius and mass that the value of g changes considerably from the top of the ionosphere to the bottom.

The second problem Triton's small radius brought about is manifest in the coordinate system. The Venus models were derived in rectangular coordinates. This may seem counter-intuitive since Venus is a sphere and hence would appear best modeled with spherical coordinates. However, the assumption that the magnetic field is uniform and straight as it impinges on the obstacle reduces the geometry to cylindrical symmetry, with the magnetic field direction taken to be the axis of the cylinder. The reason this was not used in the previous Venus and Mars studies is due to the small error introduced by substituting in the more computationally manageable rectangular symmetry. The error in approximating rectangular coordinates for intrinsically cylindrical symmetry is

proportional to the difference in radii at the top of the atmosphere as compared to the bottom. For Venus

$$\%\text{error} \propto 1 - \frac{r_B}{r_T} = 1 - \frac{6000\ \text{km}}{6300\ \text{km}} \approx 5\%$$

but for Triton

$$\%\text{error} \propto 1 - \frac{r_B}{r_T} = 1 - \frac{1352\ \text{km}}{2352\ \text{km}} \approx 43\%$$

Hence, large errors are introduced by using rectangular coordinates at Triton while small ones, roughly equivalent to computational errors [*Hoogeveen*, 1992], exist at Venus.

## V.A. Ionospheric Flow Equations

We define the cylindrical coordinate system where local vertical is in the $\hat{\mathbf{r}}$ direction, $\hat{\mathbf{z}}$ is horizontal to the planet and parallel to the magnetic field, **B**, at the top of the ionosphere, and $\hat{\phi}$ is along the corotational flow direction (figure 11).

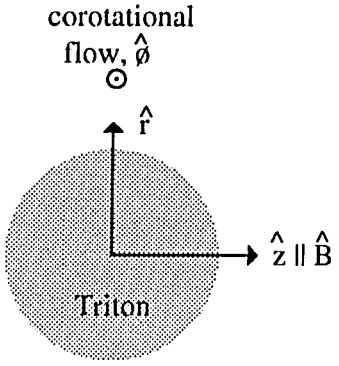


Cylindrical Coordinates

Figure 11. The coordinate system used in the flow/field model at Triton. The magnetic field lies in the +z direction, and the corotational flow lies in the $+\phi$ direction.

Having established this, we can now apply the three conservation laws to the flow: conservation of mass, momentum, and energy. The equation for the conservation of mass, also known as the continuity equation, can also describe the conservation of species particles. In this case it can be written for ions, i. In the steady state limit, this equation is written

$$\nabla\cdot(n_i\mathbf{V}_i) = p_i - l_i \equiv S_i \qquad (1)$$

where $p_i$ and $l_i$ are production and loss rates for each individual species of ion, respectively. $S_i$ is defined to be the total source rate for each species. Furthermore, $\mathbf{V}_i$

and $n_i$ are the velocity and density of each ion species, i, respectively. This implies, of course, that the total ion density is

$$n = \sum_i n_i \tag{2}$$

and the average ion mass, m, is given by

$$m = \frac{1}{n}\sum_i m_i n_i \tag{3}$$

As is evident in equation (1), the density and velocity of each species are inversely proportional, assuming that the ion source is zero. Since we require macroscopic charge neutrality, the electron density is the same everywhere as the total ion density. Therefore, in the sonic layer seen at Venus [*Cloutier et al.*, 1987], as the velocity peaks the total ion density, due to the continuity equation, must decrease proportionally. This is a distinct and clearly seen phenomena.

The conservation of momentum is very important in the flow/field model. It is this relation that embodies the transfer of momentum from the flowing plasma to the ionosphere, to the neutrals, and finally to the planet. As stated previously, the components of the momentum equation are ionospheric thermal pressure, ionospheric magnetic field, and vertical plasma flow. The steady state conservation of momentum equation can be written

$$\nabla\cdot[\rho\mathbf{V}\mathbf{V} + P] = \mathbf{J}\times\mathbf{B} + \mathbf{F} \tag{4}$$

where $\rho$ is the mass density $\rho = mn$, P is the plasma pressure tensor, **J** is the current density, **V** is the velocity defined by kinetic theory

$$\mathbf{V} = \frac{\sum_i m_i n_i \mathbf{V}_i}{\sum_i m_i n_i}$$

and **F** represents all the external forces on the plasma. These forces, or momentum losses, include the gravitational force, the collisional drag on the plasma from the neutrals, the loss in momentum due to charge exchange with the neutrals, and the loss in momentum due to recombinations. These can be written, in order, as

$$\mathbf{F} = \rho\mathbf{g} - \rho\mathbf{v}\nu_{in} - \left[\sum_i m_i(X_i + R_i)\right]\mathbf{v} \tag{5}$$

where $\nu_{in}$ is the ion-neutral collision frequency, $X_i$ is the charge exchange rate, and $R_i$ is the recombination rate all given in Table 1: Triton's Aeronomy.

The steady state equation for the conservation of energy is

$$\nabla\cdot\left[\left(\frac{1}{2}\rho V^2 + \frac{\gamma}{\gamma - 1}P\right)\mathbf{V}\right] = \mathbf{J}\cdot\mathbf{E} + Q \tag{6}$$

where $\gamma$ is the ratio of specific heats and is assumed to be $\frac{5}{3}$, **E** is the electric field, and Q is the heating done by the forces on the plasma. These heat, or energy, interactions are a very important and fundamental part of the model as revised in the *Hoogeveen* [1992] study. The study incorporated the following reactions: heating from gravitational potential energy, ion-neutral collisions, charge exchanges, and chemical and photochemical recombinations. In particular, the heating term can be written

$$Q = \rho \mathbf{g}\cdot\mathbf{V} - n_e \sum_i \nu_{in}\left[m_i V^2\left(1 + \frac{m_{ntot}}{m_i}\right)^{-1} + f\frac{3}{2}k\,(T_i - T_n)\right] + X_i\left[\frac{3}{2}kT_n - \left(\frac{1}{2}m_i V^2 + \frac{3}{2}kT_i\right)\right] - l_i\left[\frac{1}{2}m_i V^2 + \frac{3}{2}k\,(T_i + T_e)\right] \quad (7)$$

A more detailed look at each of these terms and their origins will be given in the section discussing the atmospheric chemistry at Triton. It turns out that this term, Q, is very important in detailing the specifics of the interaction with Triton.

It should be noted that equations (1) through (6) do not depend on the assumptions of MHD and are valid for any ratio of collision frequency to cyclotron frequency [*Cloutier et al.*, 1987].

Since this is a steady state model, $\nabla \times \mathbf{E} = 0$. The model also assumes the ionosphere is infinitely conducting and thus

$$\mathbf{E} = -\mathbf{V} \times \mathbf{B} \quad (8)$$

With the reasonable assumptions that the corotational flow is perpendicular to the magnetic field direction, and that the vertical flow is always downward, we can write

$$\mathbf{V} = -V_r\hat{\mathbf{r}}, + V_\phi\hat{\phi}$$

Recall that the magnetic field is along the $\hat{\mathbf{z}}$ direction. Equation (8) now becomes

$$\mathbf{E} = -\left(V_r + V_\phi\right) \times B_z = V_r B_z\hat{\phi} - V_\phi B_z\hat{r} = E_\phi - E_r \quad (9)$$

By using Ampere's Law in steady state we are able to rewrite **J** in terms of **B**

$$\mathbf{J} = \frac{\nabla \times \mathbf{B}}{\mu_0} \tag{10}$$

With this equation we can then write the joule heating term in equation (6)

$$\mathbf{J}\cdot\mathbf{E} = \left(\frac{\nabla \times \mathbf{B}}{\mu_0}\right) \cdot \left(E_\phi \hat{\phi} - E_r \hat{r}\right) = \frac{1}{\mu_0}\left[\left(-\frac{\partial B_z}{\partial r}\right) E_\phi - \left(\frac{\partial B_z}{\partial \phi}\right) E_r\right] \tag{11}$$

Let us assume the magnetic field does not change significantly in the horizontal plane. That is, the magnetic field changes more in altitude than in azimuth. This is also assumed for the gradients in density and temperature in the plasma, and is equivalent to the so called onion-skin model. The atmosphere is assumed to appear like the different layers in an onion: similar along spherical shells but not necessarily so radially. With this assumption, the last term on the right hand side of equation (11) disappears and we are left with

$$\mathbf{J}\cdot\mathbf{E} = -\frac{E_\phi}{\mu_0}\left(\frac{\partial B_z}{\partial r}\right) \tag{12}$$

The Lorentz force can also be written in this fashion, such that only B and its spatial derivative appear.

$$\mathbf{J}\times\mathbf{B} = \frac{1}{\mu_0}\left(\nabla \times \mathbf{B}\right) \times \mathbf{B} = \left(\mathbf{B}\cdot\nabla\right)\mathbf{B} - \frac{1}{2}\nabla B^2 \tag{13}$$

The first term on the right hand side of equation (13), for our geometry, is

$$\hat{z}\left(B_z \frac{\partial B_z}{\partial z}\right) = 0$$

because, again, we assume $B_z$ does not change significantly in the horizontal direction as compared to changes in the vertical direction. This leaves the last term in equation (13) which can be rewritten as

$$\frac{1}{2} \nabla B^2 = \frac{1}{2} \nabla B_z^2 = B_z \frac{\partial B_z}{\partial r}$$

Therefore, the Lorentz force term can be written simply

$$\mathbf{J} \times \mathbf{B} = - \frac{B_z}{\mu_0} \frac{\partial B_z}{\partial r} \qquad (14)$$

## V.B. Computational Solution of Equations

The three conservation equations are now in a form such that they can be solved computationally. There are five equations (three continuity, one for each species, one momentum, and one energy) with what appear to be thirteen unknowns. This does not seem to be a tractable problem. However, there are many relations which increase the number of equations and decrease the number of unknowns. The original thirteen unknowns are: $V_r$, $V_\phi$, $B_z$, $n_i$ (of which there are three species), $S_i$ (3 more), $\rho$, P, $F_r$, and Q. An examination of each one, and how it is handled, will help explain the numerical procedure for solving this complicated set of coupled equations.

1) $V_r$: The radial component of plasma velocity is an unknown. It will be solved for every step down the ionosphere. However, the initial value must be given in order for the equations to propagate. The initial value was adjusted from a value as large as Mach one to a value as small as centimeters per second.

2) $V_\phi$: The azimuthal component of velocity originates from the corotational flow. It is assumed to encounter the moon nearly sonically at the top of the ionosphere, and since the plasma is bound to the moon, is also constrained not to exceed the escape speed. The values of the escape velocity, magnetosonic velocity, and the sonic velocity at 1000 km are

$$V_{esc} = 1100 \text{ m/s}$$

$$C_{ms} = 2900 \text{ m/s}$$

$$C_s = 550 \text{ m/s}$$

which corresponds to an interesting ordering

$$C_{ms} > V_{esc} > C_s$$

Assuming the initial value of the azimuthal flow and that the only forces acting on it down the ionosphere are collisional, then the profile can be calculated

$$\rho V_\phi \frac{dV_\phi}{dr} = - \rho V_\phi \nu_{in}$$

$$\frac{dV_\phi}{dr} = - \nu_{in} \alpha n_{N_2} \alpha e^{-\frac{(r_0 - r)}{H_{N_2}}}$$

where $H_{N_2}$ is the scale height for $N_2$. This results in an exponentially decreasing horizontal velocity profile, as can be seen in figure 12. The initial value was used as a

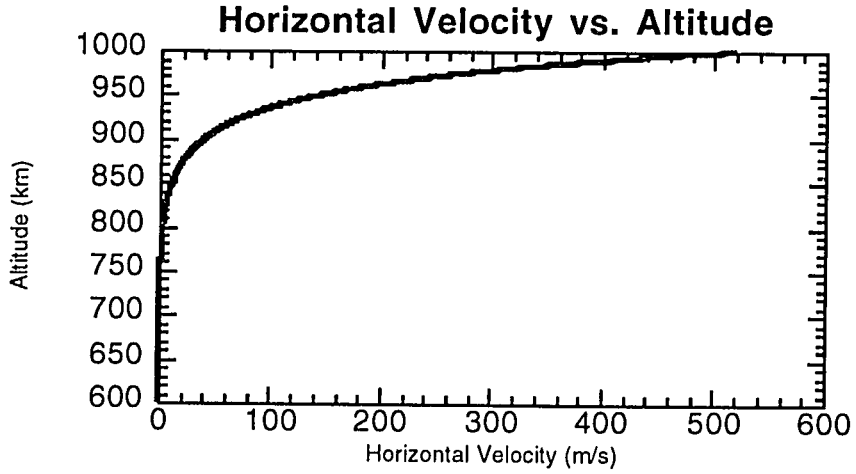


Figure 12. Plot of horizontal, or corotational, velocity versus altitude. The profile is exponentially decreasing with the molecular nitrogen scale height. The initial value was determined from a variational technique used to fit the best solution.

variational tool and ranged from the escape velocity, to the sonic velocity, to roughly 100 m/s. By use of this variational technique, we have eliminated this variable, and are left with twelve unknowns.

3) $B_z$: The magnetic field is assumed to lie in the $\hat{z}$ direction. It's magnitude is an unknown and thus solved for at every altitude step. The initial value is the only input, and is explained further shortly. It is important to note here, however, that the solution which best fit the criteria for the model, i.e., the boundary conditions, governed what the initial magnetic field was, as well as the other initial conditions. This is a general statement which explains how one chooses initial conditions, such as velocity, ion densities, and magnetic field.

4-6) $n_i$ : In the Triton model, three main ion species are assumed to exist: $H^+$, $N^+$, and $N_2^+$. Their initial values, as mentioned above, must be given. Their respective densities, after the initial input, are unknown quantities and are outputs of the model. However, there is a further requirement for these densities that has not been present in previous versions of the flow/field model. Voyager 2 has placed a constraint on the total electron density at each altitude [*Tyler et al.*, 1989]. With the natural assumption of quasi-neutrality, this model requires the sum of the three species to equal the externally specified electron density. In so doing there arises the likelihood of the necessary inclusion of a corrective term in the source rates; photoionization may not be strong enough to reproduce the high level of ionization discovered at Triton, and thus an extra production term is likely needed. This corrective term will be discussed thoroughly later.

7-9) $S_i$: The source rates, given by the algebraic sum of the production and loss rates, are arguably the most important piece to this model. The source rate can be thought

of as the sources and sinks for each ion species at each altitude range. Its dimensions are $[\text{length}]^{-3}[\text{time}]^{-1}$, which is obtained by multiplying chemical rate coefficients, $\frac{[\text{length}]^6}{[\text{time}]}$, by species densities, $[\text{length}]^{-3}$. These rates then provide the details for the individual reactions which either produce or destroy a given ion species, and will be explained in much greater detail in the section on Triton's chemistry. In any case, the source rates are known by effectively modeling the chemical reactions in the ionosphere. This reduces the number of unknowns by three, leaving nine.

10) $\rho$: The plasma density can also be written

$$\rho = \sum_i m_i n_i$$

where $m_i$ and $n_i$ refer to a particular ion species' mass, and number density, respectively. The density, $n_i$, has already been discussed. The mass, $m_i$, is known since we know which ions we are modeling. Therefore, we have reduced our unknowns by one more leaving eight.

11) P: Thermal pressure is modeled using the perfect gas law: $P = n_e k(T_i + T_e)$. The total electron density, $n_e$, has been discussed. The symbol, k, represents Boltzman's constant, leaving the ion and electron temperatures as the only possible unknowns. *Broadfoot et al.* [1989] have stated that the ionosphere of Triton is likely in thermal equilibrium with the neutral atmosphere. The neutral atmosphere functions as input to the chemical model which will be discussed further, shortly. Thus, with the neutral atmosphere used as input coupled with the assumption that the ionosphere is in thermal

equilibrium, $T_i$ and $T_e$ are known. This results in P being known and reduces the number of unknowns to seven.

12) $F_r$: The forces in the radial direction, $F_r$, also play an important role in governing the dynamics of the interaction. These forces are the means by which the momentum is transferred to the body. The forces are dependent on ion densities and velocities, and can be rewritten entirely in terms of these quantities. As a result, the vertical forces can be calculated outside the original five equations reducing the number of unknowns to six.

13) Q: The final unknown is also knowable through the aforementioned chemical analysis. The heating on the plasma is a direct result of the chemical and photochemical reactions as well as collisional heating/cooling. These terms combine to yield a calculable heating relation. However, we do not claim to model all of the possible heating mechanisms available in an atmosphere, and so include an adjustable parameter which allows further heating, or cooling, whichever the case, to allow a proper convergence of the model. With the combination of modeled heating and adjustable heat input, we have eliminated this final unknown yielding a proper match between unknowns and equations at five.

We have thus argued that a computational solution is feasible and have outlined the method by which to go about it. The next step is a further elucidation of the contributions from the atmospheric chemical reactions.

## V.C. Aeronomy

The aeronomical calculations are vital for an accurate representation of the interaction with Triton. Without the proper reactions, the specific interplay among the flowing plasma and the stationary neutrals could not be modeled, and the entire attempt would be too general for any real meaning. Not only do the chemical reactions give information concerning the rates of production and loss of the ion species, thereby allowing a calculation of the density changes of the ion species, but the aeronomy also allows calculation of the forces and the heating done on the plasma by the neutrals. There are four basic reactions modeled in the chemistry section of the flow/field model: photoproduction, ion-neutral collision, charge exchange, and recombination. Each type of reaction contributes differently to all three model parameters: source, force, and heat.

Photoproduction affects the source term in an obvious way. For a photoproduction rate of $Ph_i$, the source term, S, gets incremented

$$\Delta S = \sum_i Ph_i$$

which is a summation of all species' individual photoproduction rates, where the subscript i refers to each species of ions. Photoproduction has no forcing effect on the plasma since we assume the neutral particle to be initially stationary and therefore devoid of any possible momentum. However, photoproduction does add heat to the plasma

$$\Delta Q = \sum_i \frac{3}{2} k T_n \, Ph_i$$

where $T_n$ is the neutral temperature. As mentioned in the introduction and as will be discussed in the results section, the photoproduction rate at Triton is small, and therefore affects these three terms minimally.

Ion-neutral collisions have no effect on the source term. When an ion collides elastically with a neutral there is no change in the composition of either the plasma or the neutrals. On the other hand, both the force and the heat terms are affected and play important roles in the transfer of flow at low altitudes. A collision causes a net loss in momentum in the plasma since we assume a flowing ion strikes a stationary neutral and loses all of its flowing momentum

$$\Delta F_r = - \sum_i \rho_i V_{ri} \nu_{in}$$

A collision also causes a loss in the plasma's total heat, or energy. Ordinarily, when the plasma is considered to be hotter than the neutral atmosphere (e.g., Venus), there is a loss due to a thermalization between the two particles. In the case of Triton, however, recall that the ionospheric plasma and the neutral atmosphere are in thermodynamic equilibrium [*Broadfoot et al.*, 1989] and hence there is no heat gain or loss from this term. However, there is still an energy loss in a collision. We assume the ion is flowing and, after the collision, has lost this ordered flow and hence has lost kinetic energy

$$\Delta Q = - \sum_i \nu_{in} m_i v^2 \left[ 1 + \frac{m_{ntot}}{m_i} \right]^{-1}$$

This result was obtained by solving the conservation of momentum and energy equations for a moving ion of mass, $m_i$, and a stationary neutral of mass, $m_{ntot}$, which is simply the average mass of the neutrals present at that altitude.

There is no net change in total plasma density for a charge exchange process, and thus there is no contribution to the source term. A charge exchange does exchange momentum, because the ion lost in the exchange continues on with its velocity, and hence momentum, but the ion gained brings in no ordered flow since it was formerly a stationary neutral. The decrement in force on the plasma for the generic charge exchange

$$A + B^+ \rightarrow A^+ + B$$

is given by

$$\Delta F_r = - \sum_{A,B} X_{AB} m_B V_r$$

There is also a change in plasma heat for a charge exchange due to (a) the addition of the thermal energy from the neutral, and (b) the subtraction of both the kinetic and thermal energy from the ion. This can be written as

$$\Delta Q = \sum_{A,B} X_{AB} \left[ \left( \frac{3}{2} k T_A \right) - \left( \frac{3}{2} k T_B + \frac{1}{2} m_B V^2 \right) \right]$$

Since the temperatures for the neutrals and the plasma are equal in the ionosphere of Triton, this reduces to

$$\Delta Q = - \sum_{A,B} X_{AB} \left( \frac{1}{2} m_B V^2 \right)$$

Representing that the heat loss is due only to the loss in kinetic energy form the flowing ion.

Recombination, as the name implies, is the process which takes an ion and an electron, combines them, and makes one neutral particle. This obviously is a loss, or a sink, and thereby contributes to the overall source term. In a similar way to a collision, the recombination of an ion subtracts the ion's momentum from the flow, as well as both its kinetic and thermal energies. These modifications to the source, momentum, and energy equations can be written as follows

$$\Delta S = - \sum_i R_i$$

$$\Delta F_r = - \sum_i R_i V_r$$

$$\Delta Q = - \sum_i R_i \left( \frac{1}{2} m_i V^2 + \frac{3}{2} k (T_i + T_e) \right)$$

The following is a list of chemical reactions used in modeling the ionosphere of Triton:

**Table 1: Triton's Aeronomy**

| Ref | Reaction | Result | Rate | Type |
|---|---|---|---|---|
| a | $N_2 + e \rightarrow$ | $N_2^+ + 2e$ | $8.0 \times 10^{-17}$ | Impact |
| a | $N_2 + e \rightarrow$ | $N + N^+ + 2e$ | $2.0 \times 10^{-17}$ | Impact |
| b | $N_2 + h\nu \rightarrow$ | $N_2^+ + e$ | $5.4 \times 10^{-10}$ | Photo |
| b | $N_2 + h\nu \rightarrow$ | $N + N+ + e$ | $6.7 \times 10^{-11}$ | Photo |
| c | $N_2^+ + N \rightarrow$ | $N_2 + N^+$ | $1.0 \times 10^{-11}$ | Exchange |
| c | $N_2^+ + H_2 \rightarrow$ | $N_2H^+ + H$ | $1.7 \times 10^{-9}$ | Recomb |
| b | $N_2H^+ + e \rightarrow$ | $N_2 + H$ | $5.0 \times 10^{-7}$ | ination |
| c | $N^+ + H_2 \rightarrow$ | $NH^+ + H$ | $7.0 \times 10^{-10}$ | Recomb |
| c | $NH^+ + e \rightarrow$ | $N + H$ | $2.0 \times 10^{-7}\left(\frac{T}{300}\right)^{0.5}$ | ination |
| b | $N^+ + H \rightarrow$ | $N + H^+$ | $1.9 \times 10^{-10}$ | Exchange |
| c | $N_2^+ + e \rightarrow$ | $N + N$ | $1.8 \times 10^{-7}\left(\frac{T}{300}\right)^{-0.39}$ | Recomb. |
| c | $N^+ + e \rightarrow$ | $N + h\nu$ | $3.8 \times 10^{-12}\left(\frac{T}{300}\right)^{-0.62}$ | Recomb. |
| c | $H^+ + e \rightarrow$ | $H + h\nu$ | $3.5 \times 10^{-12}\left(\frac{T}{300}\right)^{-0.7}$ | Recomb. |
| e | $H^+ + N_2 \rightarrow$ | $N_2^+ + H$ | $4 \times 10^{-17}$ | Exchange |
| d | | $\nu_{in}$ | $2.6 \times 10^{-9}\frac{[n_i + n_n]}{\sqrt{M}}$ | Collision |

Table 1. A list of ion and neutral chemistry used in the flow/field model. Rates are in units of $s^{-1}$, $cm^3\ s^{-1}$, and $cm^2$ for dissociative, two-body reactions, and references (a) and [e], respectively. References are (a) *Krishnakumar et al.* [1990]; (b) *Kirby et al.* [1979] and *Wu et al.* [1984] and *Morioka et al.* [1984]; (c) *Prasad and Huntress* [1980]; (d) *Hanson* [1961].; and [e] *Monnom et al.* [1975].

### V.D. Analytical Solutions and Extra Production Rate

Using the aforementioned geometrical assumptions and conservation equations, a solution to the coupled equations can be attained. Ordinarily, the continuity equation is used to find the change in ion density in altitude. This was the case for the previous

versions of the flow/field model. However, due to the nature of the data from Voyager 2, we know the total electron density profile, and hence the total ion density profile, throughout the atmosphere of Triton. Formerly, each individual ion species' density was measured, i.e., by Pioneer Venus. Furthermore, the chemistry, including the exact ion production rates, were well known at Venus allowing a simple, but yet complete, model of the chemical processes in the atmosphere. At Triton this is not the case. There is such a large ion density that there must be an additional ionizing source in the ionosphere other than photoionization. Since this is an unknown mechanism its rate cannot be modeled with great confidence. Therefore it makes the most sense to assume the total ion density and solve for the unknown ion production rate. This is what is done with the continuity equation. Instead of solving for $n_e$, we assume it and all other terms are known, with the exception of this missing production term, $P_p$. This extra ionization is likely impact ionization from precipitating electrons [*Strobel et al.*, 1990a], and hence the meaning of $P_p$: Production from precipitation.

To calculate the extra production rate, $P_p$, an added unknown, we need to add one more equation. This equation is simply the condition for quasi-neutrality

$$n_e = \sum_i n_i$$

Since $n_e$ is known from experimental data onboard Voyager 2, we have added an equation without adding an unknown. We now have six equations and six unknowns; equal once again. Therefore we are able to solve for $P_p$, $V_r$, $n_{H^+}$, $n_{N^+}$, $n_{N_2^+}$, and $B_z$. The solutions must follow this order since, as you can see in equations (21) though (23), the magnetic field depends on the densities and the velocity; the densities depend on the velocity; and the velocity depends on the exact production rate.

In order to solve the six equations discussed previously, one must find $P_p$ first. We begin by defining the drift velocity as

$$\mathbf{V_D} = \frac{\mathbf{E} \times \mathbf{B}}{B^2} = -\frac{E_\phi \times B_z}{B_z^2} = -\frac{E_\phi}{B_z}\hat{r} \tag{15}$$

the total velocity by

$$V_T = \sqrt{V_r^2 + V_\phi^2}$$

as well as a couple of other terms

$$\begin{aligned} \#1 = V_D F_r + Q\frac{dn_e}{dr}\left(mV_D V_r^2 + \frac{1}{2}mV_r V_T^2\right) - \frac{dP}{dr}\left(V_D + \frac{\gamma}{\gamma - 1}V_r\right) - \rho V_\phi V_r \frac{dV_\phi}{dr} \\ - \frac{\rho}{r}\left[V_D\left(V_r^2 - V_\phi^2\right) + \frac{1}{2}V_T^2 V_r - \frac{\gamma}{\gamma - 1}(P_{Tot})\,V_r\right] \end{aligned} \tag{16}$$

and

$$\#2 = \frac{1}{2}\rho V_T^2 + \rho V_r^2 - \frac{\gamma}{\gamma - 1}P_{Tot} + 2\rho V_D V_r \tag{17}$$

where r is the distance from the center of the moon to the altitude at which the calculation takes place

$$r = R_0 + \text{altitude}$$

$R_0 = 1352$ km is the radius of the moon; and $P_{tot}$ is given by

$$P_{Tot} = nk(T_i + T_e) + P_{miss} \tag{18}$$

Furthermore, if $n_e$ is known at all altitudes, one can solve numerically for $\frac{dn_e}{dr}$

$$\frac{dn_e}{dr} = \frac{n(r+h) - n(r)}{h} \tag{19}$$

where h is the step size. It was found that the optimum step size for this calculation was 5 km [*Hoogeveen*, 1992]. Combining equations (1) and (4) with definitions (15) through (19), the extra production required above and beyond those considered by ordinary chemistry can be solved for

$$P_p(r) = \frac{\left[\left(\frac{\left(S_i - \frac{dn_e}{dr}V_r\right)}{n_e} - \frac{V_r}{r}\right)\#2 - \#1\right]}{\left[\left(\frac{3}{2}kT_i + \Phi_{II}\right) - \frac{\#2}{n_e}\right]} \tag{20}$$

This extra production rate obviously affects the source terms for the ions, but it also affects the heating done to the plasma. An impact ionization is, for all intents and purposes, exactly like a photoionization. The rates are, of course, different, but the effects are the same. Both add number to the plasma, and both heat it by adding the thermal energy of the former neutral to the plasma. Furthermore, both mechanisms contribute additional heating, denoted by $\Phi_{II}$ for the impact ionization, if the ionizing agent, either the photon or the electron, has sufficiently greater energy than the ionization energy of the neutral. All of this is taken into consideration by adding the following to Q from the chemistry

$$\Delta Q = P_p \sum_i \frac{3}{2} k T_i + \Phi_H$$

Incidentally, just as in the case of the photoionizations, the impact ionizations have no effect on the total momentum change in the plasma. That is

$$\Delta F_r = 0$$

from the extra production term, $P_p$.

The vertical velocity is solved for next. Given the full set of values for the altitude just above the one being calculated, as well as S, F, and Q, including $P_p$, the velocity is well defined. By defining a group of terms labeled $V_{coef}$ to simplify the equation

$$V_{coef} = V_D \frac{\left(V_r^2 - V_\phi^2\right)}{r} + V_r V_\phi \frac{dV_\phi}{dr} + \frac{1}{2} V_T^2 \frac{V_r}{r} \tag{21}$$

we can write the differential vertical velocity as equation (22 below)

$$\frac{dV_r}{dr} = \frac{F_r V_D + Q - \frac{dn_e}{dr}\left[m V_r^2 V_D + \frac{1}{2} m V_T^2 V_r\right] - \frac{dP_{Tot}}{dr}\left(V_D + \frac{\gamma}{\gamma - 1} V_r\right) - \rho V_{coef} - \frac{\gamma}{\gamma - 1}\frac{V_r}{r} P_{Tot}}{\left(\frac{1}{2}\rho V_T^2 + \frac{\gamma}{\gamma - 1} P_{Tot} + \rho V_r^2 + 2\rho V_D V_r\right)}$$

The individual ions have their own sinks and sources one of which is the extra term $P_p$. The only information received from the calculation of $P_p$ is the total contribution to the source term, S, not the individual $S_i$'s. The contribution to each species must be

considered. According to Table 1, if $P_p$ is indeed impact ionization from precipitating electrons, then the contributions from $P_p$ to each species is known. As seen in the first two entries in the table, when a superthermal electron of energy 20 keV, as reported by *Mauk et al.* [1994], impacts on $N_2$, the dominant neutral molecule in the atmosphere, then 20% of the reactions yield $N^+$. The rest of the impact ionizations, 80%, produce $N_2^+$ ions [*Krishnakumar et al*, 1990]. This is very important to note due to some disagreement regarding the effectiveness of creating $N^+$ versus creating $N_2^+$ from impact ionization on $N_2$. In any event, the species' density is now written

$$\frac{dn_i}{dr} = \frac{1}{V_r}\left[S_i - \left(\frac{dV_r}{dr} + \frac{V_r}{r}\right)\right] \tag{23}$$

in which the correct proportion of $P_p$ for each species appears in the $S_i$ term.

The magnetic field equation is solved next. The differential equation for $B_z$ is written

$$\frac{dB_z}{dr} = \frac{\mu_0}{B_z}\left[F_r - mV_r^2\frac{dn_e}{dr} - \rho\left(2V_r\frac{dV_r}{dr} + \frac{V_r^2 + V_\phi^2}{r}\right) - \frac{dP_{Tot}}{dr}\right] \tag{24}$$

From Ampere's Equation we know that a change in magnetic field resulting from a change in spatial dimensions is caused by a current. Ampere's Equation in Triton's ionospheric geometry was given by equation (10)

$$\nabla \times \mathbf{B} = \mu_0 \mathbf{J} \rightarrow J = \frac{-1}{\mu_0}\frac{dB_z}{dr}$$

Equation (24) rewritten in this form clearly illustrates how each force on the left-hand side contributes to the global current system which affects the magnetic field magnitude

$$\frac{-1}{\mu_0}\frac{dB_z}{dr} = \frac{-1}{B_z}\left[F_r - mV_r^2\frac{dn_e}{dr} - \rho\left(2V_r\frac{dV_r}{dr} + \frac{V_r^2 + V_\phi^2}{r}\right) - \frac{dP_{Tot}}{dr}\right] \qquad (25)$$

The first term on the right hand side in equation (25) is the vertical component of forces on the plasma composed of ion-neutral collisions and various other momentum exchanges discussed in the chemistry section. The second and third terms are currents associated with a change in the inertia of the plasma, $\frac{d}{dr}(\rho V^2)$. The final current is due to changes in the total pressure. These three currents dominate at different altitudes, respectively, and therefore cause the magnetic field magnitude to rise and fall accordingly.

**V.E. Initial Conditions**

An important step in the model is the establishment of the proper initial conditions. If the initial velocity, magnetic field, and densities are not in the correct regime, the model will not converge. This implies that the true initial conditions at the top of the ionosphere, accepted to be 1000 km, will be the only conditions for which the model converges. In truth, they may not be the only conditions that work. However, coupled together with such physical restraints as observed ion densities, and velocities smaller than Mach one, a valid set of initial conditions can be found. Furthermore, we know that the total pressure must be conserved as one crosses from the undisturbed magnetosphere through the interaction region and into the atmosphere of Triton. This relation can be represented by

$$P_{mag} = P_{iono}$$

or, more explicitly

$$\frac{B^2_{mag}}{2\mu_0} + \rho V^2_{mag} + [n_e k(T_i + T_e)]_{th\ mag} + P_{sth\ mag}$$
$$= \frac{B^2_{iono}}{2\mu_0} + \rho V^2_{iono} + [n_e k(T_i + T_e)]_{iono} + P_{sth\ iono}$$

where "th" denotes the thermal component, and "sth" denotes the superthermal, or hot component in either Neptune's magnetosphere, "mag", or in Triton's ionosphere, "iono." Recall that conditions in the magnetosphere were observed by Voyager 2's instruments and suggest the flow striking Triton is supersonic and sub-Alfvénic. Recent work by *Mauk et al.* [1994] demonstrates the hot component in the magnetosphere has a significant pressure and must be taken into consideration when calculating the pressure transfer. This results in the following ordering

$$\frac{B^2_{mag}}{2\mu_0} > \rho V^2_{mag} \approx P_{sth\ mag} > [n_e k(T_i + T_e)]_{th\ mag}$$

which is different than the ordering at Venus. This relation implies the magnetic field, as it crosses the shock region (be it fast mode or Alfvén wing), cannot magnify greatly. Most of the incident pressure resides in the magnetic field and thus there is little excess pressure to transfer to, and increase the ionospheric magnetic field. This constraint forces the magnetic field to be within a set range of values at 1000 km.

Putting in the numbers for the magnetospheric plasma:

$$B_{mag} = 8\ nT\ [Ness,\ 1989]$$

$$\rho_{th\,mag} = \left(m_p\, 0.07 \neq cm^{-3} + m_{N^+}\, 0.04 cm^{-3}\right) = 1.05 \times 10^{-21} \frac{kg}{m^3} \text{ [Belcher et al., 1989]}$$

$$P_{sth\,mag} = 2 \times 10^{-12} \frac{N}{m^2} \text{ [Mauk et al., 1994]}$$

$$V = 42.9 \frac{km}{sec};\ n_{emag} = (0.07 + 0.04)\ cm^{-3} = 1.1 \times 10^5\ m^{-3}$$

$$T_i = \frac{0.07\, T_p + 0.04\, T_{N^+}}{1.1};\ T_e = 30\ eV$$

where $T_p = 7$ eV and $T_{N^+} = 60$ eV [*Belcher et al.* 1989]

When all things are then calculated, the ordering

$$\frac{B^2_{mag}}{2\mu_0} > \rho V^2_{mag} \approx P_{sth\,mag} > [n_e k(T_i + T_e)]_{th\,mag}$$

is numerically

$$2.5 \times 10^{-11} > 1.5 \times 10^{-12} \approx 2 \times 10^{-12} > 1.6 \times 10^{-13} \qquad (26)$$

all in mks units of N $m^{-2}$.

The numbers in equation (26), coupled with the Radio Science Experiment's occultation results, allow us to specify the ionospheric initial conditions . Recall that the RSS observed a total electron density through the atmosphere of Triton. Figure 13 shows the most reliable results begin at the top of the ionosphere, or 1000 km. This added restraint forces the densities to some range of values. If, however, we assume that $N^+$ is the dominant ion, as will be shown later, then this range of values collapses to a known

number. Furthermore, if we force the initial velocity to be subsonic all initial conditions are then specified.

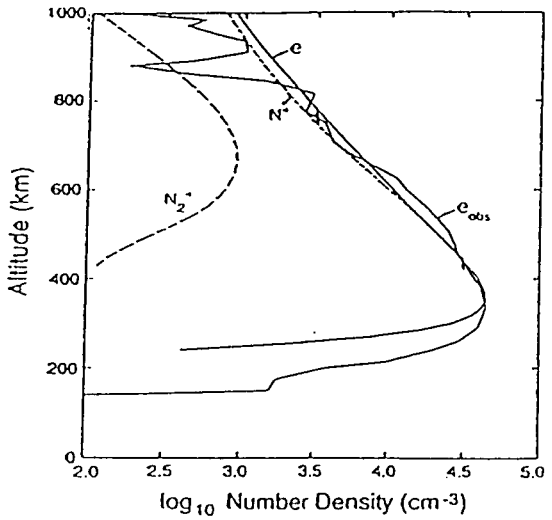


Figure 13. Measured electron number densities. This plot is taken from *Yung and Lyons* [1990] and thus also shows their calculated values. However, the $e_{obs}$ profile was first reported by *Tyler et al.* [1989], and is the profile of interest here.

The values reported above can be used to calculate a valid initial magnetic field. The equation is

$$B_{\substack{iono \\ ini}} = \left[ B_{mag}^2 + 2\mu_0 \left( \begin{array}{c} \rho V^2_{mag} + [n_e k(T_i + T_e)]_{mag} + P_{sth\ mag} \\ - \rho V^2_{iono} - [n_e k(T_i + T_e)]_{iono} - P_{sth\ iono} - (\rho g dr)_{iono} \end{array} \right) \right]^{\frac{1}{2}}$$

The resultant magnetic field ranges from a maximum value of 8.02 nT, corresponding to a negligible initial ionospheric velocity of < 1m/s, to a minimum value of 7.64 nT, corresponding to the greatest possible initial ionospheric velocity of Mach one. The initial values of both velocity and magnetic field thus range for each run, and the one which allows for the proper convergence of the code is deemed the solution.

## VI. Results

The interaction between Neptune's corotating magnetosphere and Triton has been defined and explained. In this section the results from the model method are discussed. If our model is able to reproduce the observed characteristics of this interaction, as recorded by Voyager 2, while obeying the requisite physical laws, the solution to the flow problem is found.

As mentioned previously, there are different theories as to the exact content and nature of Triton's atmosphere. This study does not wish to repeat those studies but rather uses a unique approach to the plasma flow aspect of the problem. Therefore we have, without prior bias, adopted three independent models for Triton's atmosphere and used them to solve the plasma interaction. For each neutral model, we (a) extracted model densities and temperatures and used them as input for our model, (b) executed a best-solution study for initial vertical and horizontal velocities, (c) executed a best solution study for the ratios of initial ion abundance, i.e., the amounts of $N^+$, $H^+$ and $N_2^+$ at 1000 km altitude, and (c) recorded the behavior of the various plasma parameters.

The three models used were taken from the following representative studies: (a) the *Broadfoot et al.* [1989] initial study of the UVS experiment in which they concluded $N_2$ to be the dominant neutral species at a thermospheric temperature of 95 K, (b) *Summers and Strobel* [1991] in which a photochemical analysis resulted in the hypothesis that there existed substantial N densities, as well as non-negligible amounts of H and $H_2$, and (c) the most recent, and perhaps most complete study on the neutral atmosphere, performed by *Krasnopolsky et al.* [1993] in which the UVS data was reanalyzed and absorption features attributable to atomic nitrogen were found, and included with

plausible profiles of H and $H_2$. The final runs, those which satisfy best the requisite criteria, both numerical and physical, are reported below.

## Flow/Field Results Using Broadfoot et al. Neutrals

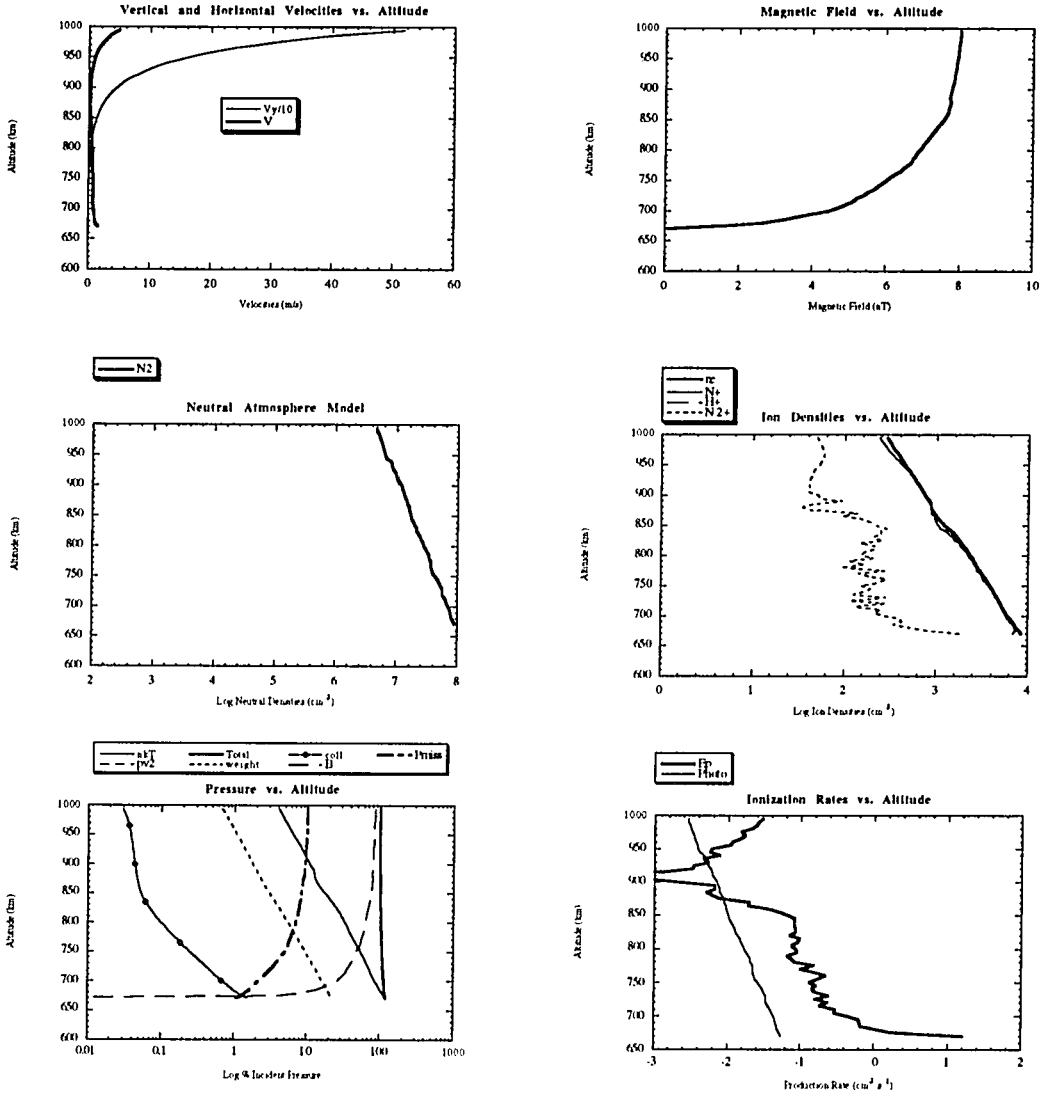


Figure 14. Flow/field results using the *Broadfoot et al.* [1989] neutral atmosphere. The six panels show the behavior of all calculated values. Of particular interest are the $N_2^+$ profile, the intersection of the magnetic pressure curve with the collision curve (discussed in the text), the extra production rate (ep), and finally, the altitude where the flow stops.

## Flow/Field Results Using Summers and Strobel Neutrals

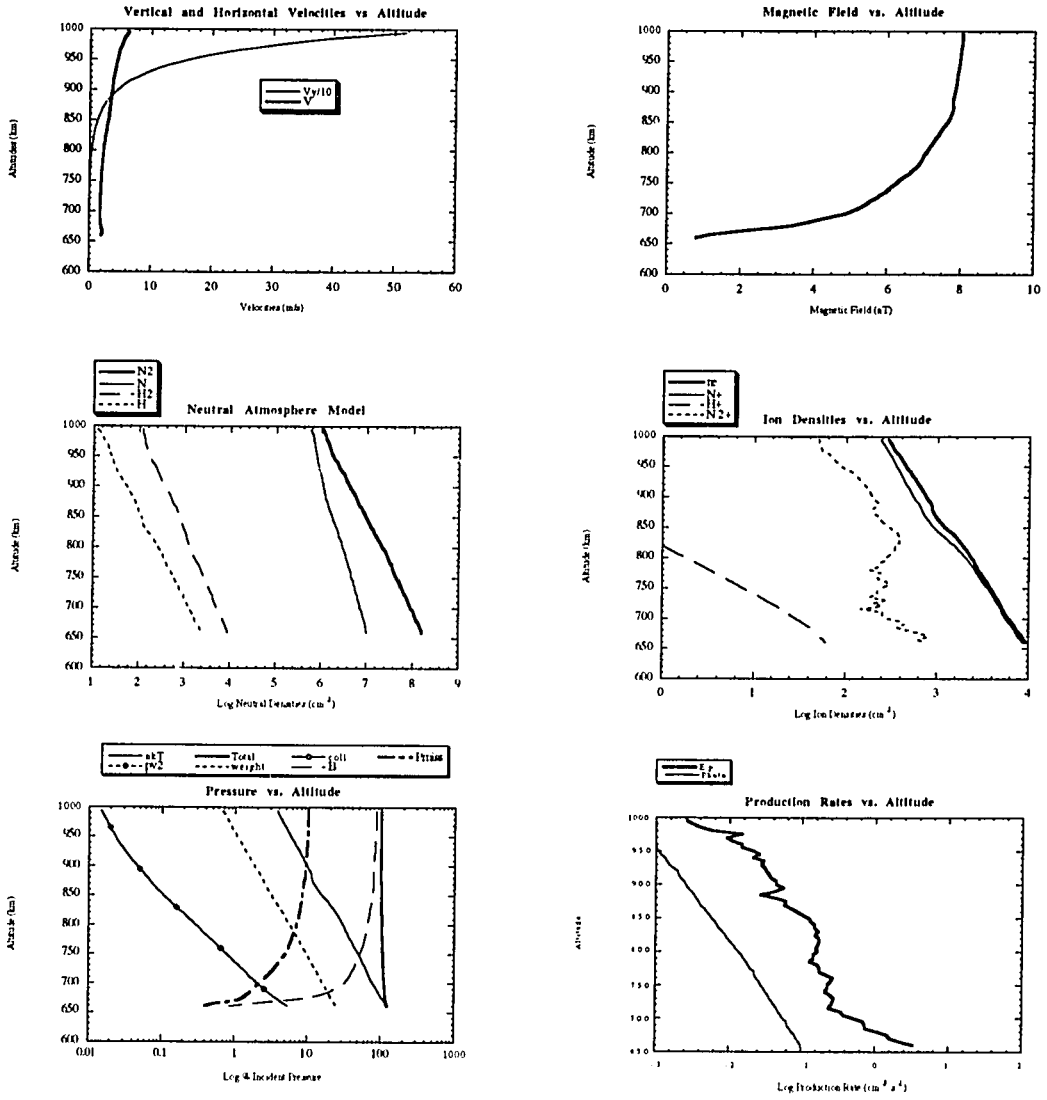


Figure 15. Flow/field results using the *Summers and Strobel* [1991] neutral atmosphere. Refer to the caption under Figure 14 for comments regarding the interesting aspects of these figures.

## Flow/Field Results Using Krasnopolsky et al. Neutrals

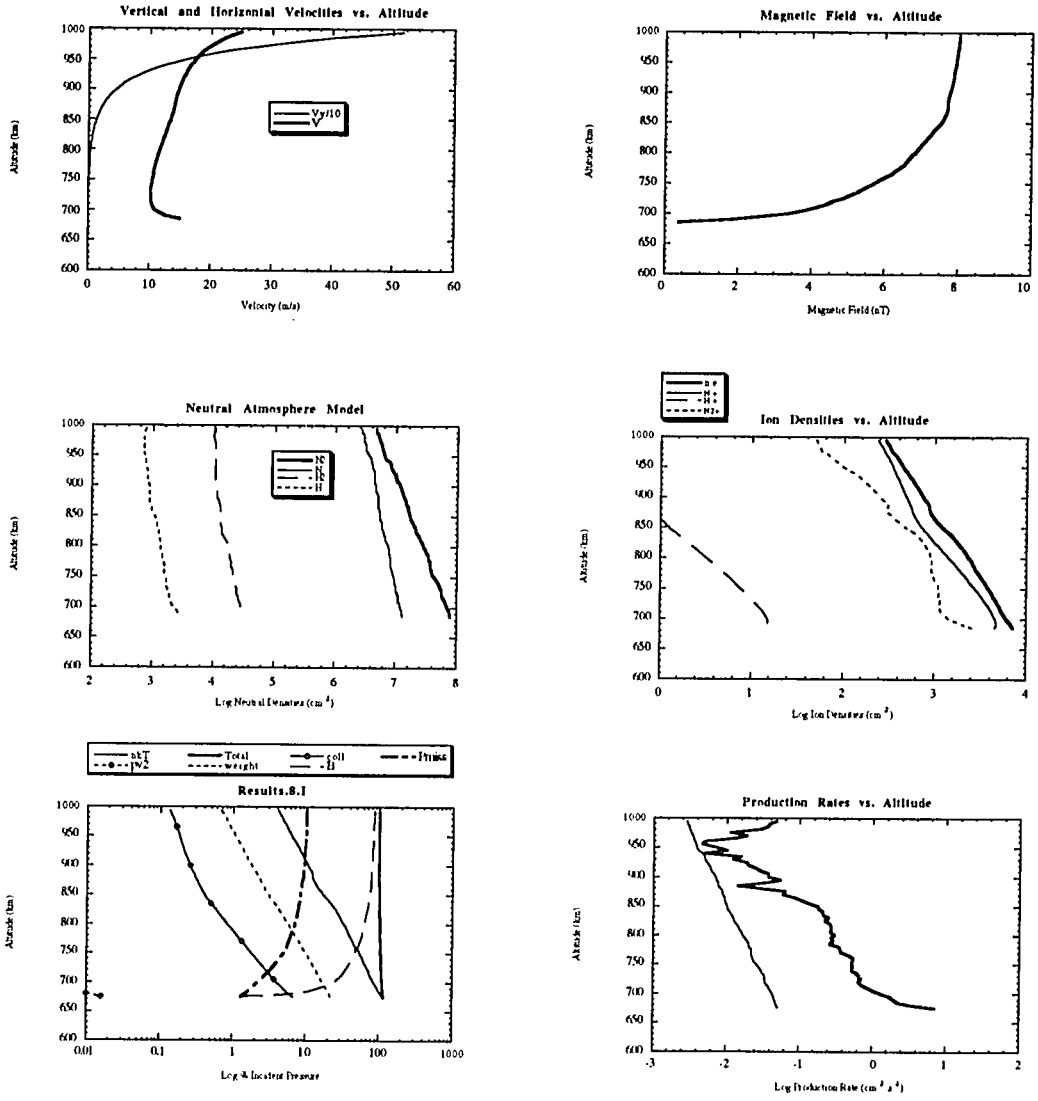


Figure 16. Flow/field results using the *Krasnopolsky et al.* [1993] neutral atmosphere. Refer to the caption under Figure 14 for comments regarding the interesting aspects of these figures.

## VII. Discussion

### VII.A. Similarities

The first similarity noticed in figures 14 through 16 is that in all three runs the initial horizontal velocity which best fit the models was approximately 520 m/s. This corresponds to a Mach number of just less than one. This is entirely reasonable and to be expected when one realizes that the model is forced to obey data taken during occultation, at sub-flow angles of nearly $\pm 90°$. In the Venus interaction, the flow near the terminators just above the ionopause is nearly Mach one [*Brace et al.*, 1983], thereby reinforcing our assertion that the interactions are similar in nature.

It is also apparent in all three models that $N^+$ is the dominant ion at 1000 km. In order to demonstrate the process by which this is concluded, notice in figure 17 the rapid increase in $N^+$ in the first 50 km. This sharp "ramping" of ion densities in the initial 50 km is a sure sign that the initial condition, $N_2^+ > N^+$, is incorrect. Even though $N^+$ must be dominant for the three models, the exact ratios for each model differs at lower altitudes, as will be discussed in the "differences" section.

Another obvious similarity in the three models is the superthermal pressure, or Pmiss, profile. The superthermal population is tied closely to the extra production rate; the superthermal magnetospheric electrons are ionizing Triton's neutral atmosphere through impact ionization. Therefore, insofar as the extra production profiles are similar, the superthermal pressure profiles are similar. And in fact, since the superthermal population is so energetic, small deviations in the extra production term affect the total superthermal population minimally. Therefore, even though the three extra production profiles may differ by as much as an order of magnitude at some altitudes, this does not

affect the superthermal pressure greatly, thereby explaining the similarity in the three pressure profiles.

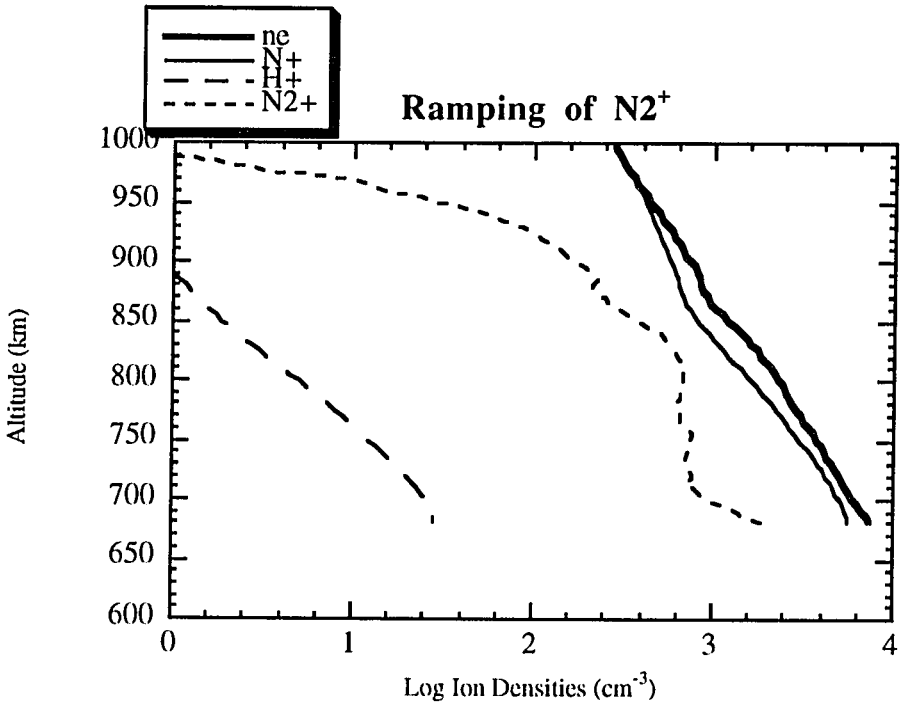


Figure 17. Ramping of $N_2^+$. Notice the sharp increase in $N_2^+$ number density in the first 50 km. This indicates an incorrect initial value assumption, and therefore must be changed.

The details of pressure transfer are another important similarity in the pressure profiles in figures 14-16. Notice that for each model, the total pressure remains somewhat constant and, perhaps even increases slightly, as the plasma flows down the atmosphere. According to the criteria adopted in the Venus and Mars interactions, this would indicate that the flow has not transferred its momentum, i.e., pressure, to the obstacle. However, further analysis of the pressure graphs details a different possibility. Previously the model was required to transfer the flowing momentum through the ionosphere directly to the neutrals resulting in an ionosphere in hydrostatic equilibrium.

Recall that hydrostatic equilibrium occurs when the gravitational force equals the thermal pressure

$$dP = -\rho g dr$$

This condition would be graphically represented in the Pressure Panel in figures 14-16 if the weight curve intersected the thermal pressure curve. This does not happen at any altitude in any of the three models. Therefore we conclude that the ionosphere is not in hydrostatic equilibrium when the flow stops. This is fundamentally different from the models at Venus and Mars [*Cloutier et al*, 1987; *Stewart*, 1991]. Furthermore, the ionosphere cannot be in hydrostatic equilibrium anywhere above the peak ion density. This is obvious as demonstrated by the parallel nature of the weight curve and the thermal pressure curve in all the Pressure Panels of figures 14-16; they cannot cross until the thermal pressure curve turns over after the peak has been reached.

If the ionosphere is not in hydrostatic equilibrium above the peak, what happens to the excess pressure from the incident flow? Since the majority of the incident pressure resides in the magnetic field (approximately 80-90%, a significant difference in the character of the flow at Triton as compared to Venus), then in order for this excess pressure to transfer to the neutrals, the following condition must occur

$$\frac{B^2}{2\mu_0} \rightarrow \int_{\text{top of iono}}^{\text{xalt}} \rho V \nu_{in} dr$$

where xalt refers to the altitude at which the pressure is transferred. An examination of figures 14-16 shows that this occurs nearly simultaneously with the flow shutting off, i.e., when the velocities and the magnetic field go to zero. Thus the flowing pressure is

transferred to the neutrals in all three models, with the realization that the ionosphere is not in hydrostatic equilibrium at this point. Again, while the different models all agree the pressure gets transferred, each differs slightly regarding the exact altitude at which this occurs.

Finally, it is important to notice where the flow shuts off in all three models. In Broadfoot et al.'s 1989 paper examining the UVS data, they conclude the exobase exists at an altitude of 750 km. The more recent and thorough analysis of the neutral atmosphere by *Krasnopolsky et al.* [1993] estimates the exobase to be at 870 km. For a plasma interacting with a non-magnetized obstacle, theory predicts that the flow will shut off within a scale height of the exobase. As seen in figures 14-16, the flow shuts off at an altitude of 675 ± 20 km in all three cases. One can calculate the neutral scale height at both the reported exobases, 750 km and 870 km, to be

$$H_e = \frac{kT}{mg} = \frac{kT(R_0 + r)^2}{GM_I m_{N_2}}$$

Using the appropriate values, the exobase scale heights are

$$H_e(750\text{ km}) = 95\text{ km}$$
$$H_e(870\text{ km}) = 106\text{ km} \qquad (27)$$

These values suggest that if 750 km is the exobase, the flow should stop around 750-95 = 655 km; if the exobase is at 870 km altitude, then the flow should stop around 870-106 ≈ 760 km altitude. Figures 14-16 suggest the exobase is at an altitude closer to 750 km rather than 870 km.

## VII.B. Differences

It is primarily evident that the differences between the three models are not significant. The only important differences are the behaviors of the ion densities throughout the ionosphere, and to a lesser degree, the behavior of the vertical velocity. In order to further elucidate the differences in the models, the extra production profile was made the same for all three models. This was accomplished by setting the extra production profile to twenty times the photoproduction rate, a scheme justified by closer examination of the Production graphs in figures 14-16. The model was then modified to solve for $V_r$, $B_z$, and $n_i$ not forcing obedience to the observed electron density profile. The three adjusted model results appear in figures 18 through 20.

By comparing figures 18-20 and figures 14-16 we are able to see some small differences. First of all, the Summers and Strobel neutrals force the flow to stop at an altitude of 680 km, the Krasnopolsky et al. neutrals force the flow to stop just below 650 km, and an atmosphere of only N2 stops the flow at an altitude of 660 km. The initial velocities range from -23 m/s for Krasnopolsky neutrals to -9 m/s for Summers and Strobel neutrals. Finally, the most important difference, is that this adjusted equal production rate forces greater ion densities than observed for the neutral models of Krasnopolsky et al. and Broadfoot et al., and less ion densities for the Summers and Strobel neutrals. This implies that the Summers and Strobel atmosphere requires a greater integrated flux of precipitating electrons to reproduce the observed ionosphere than either the N2 only atmosphere of Broadfoot et al. or the neutral model put forth by Krasnopolsky et al.

## Results Using Exponential Extra Production Rate for Broadfoot et al. Neutrals

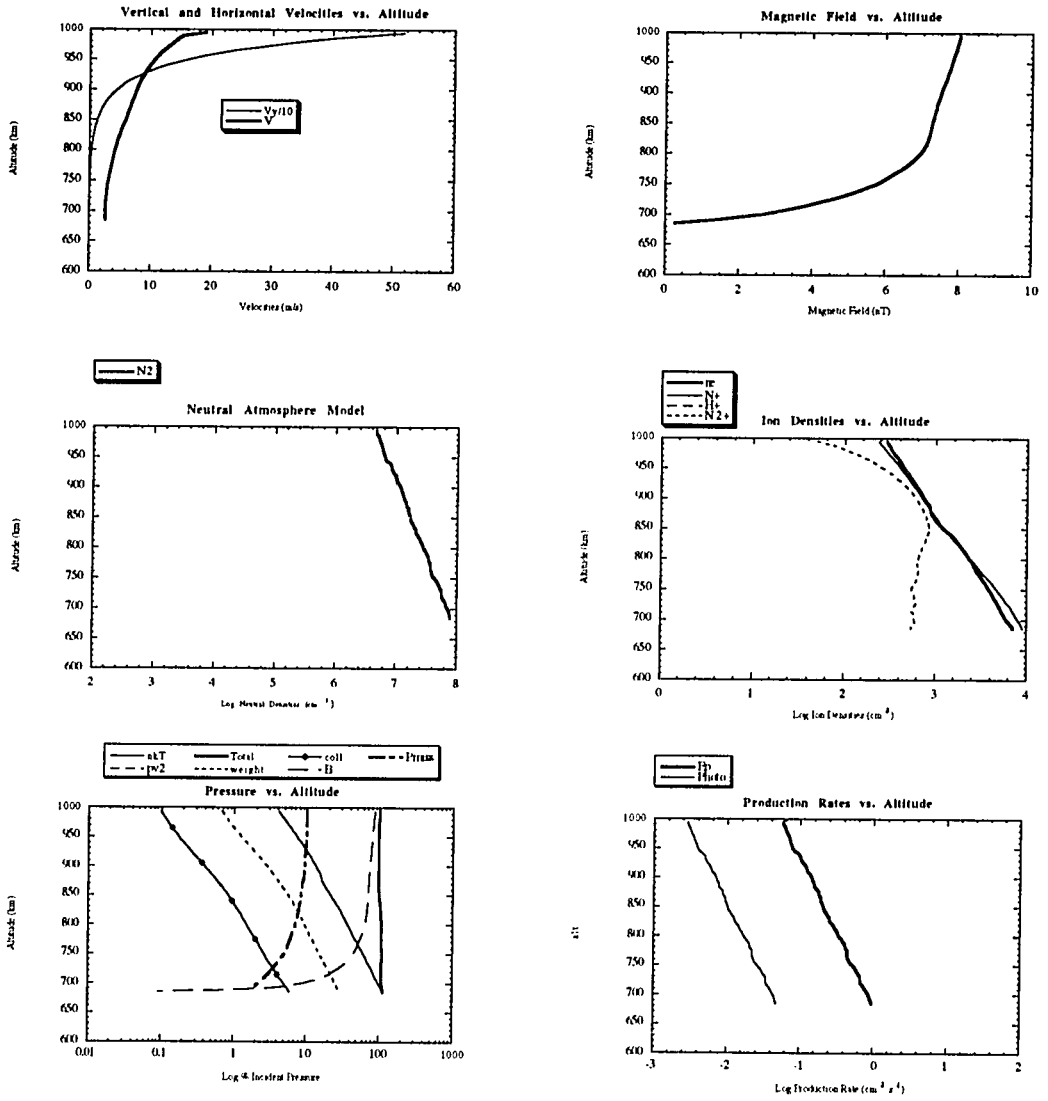


Figure 18. Flow/field results with *Broadfoot et al.* [1989] neutrals when the extra production rate is assumed to follow the neutral density profile. Notice in the bottom right panel the extra production rate (Ep) runs parallel to the photoionization rate (Photo); both profiles follow the scale height of the neutral density, shown in the left center panel. Note here that the total ion density is larger than the electron density at altitudes around 850 km (see text for discussion).

## Results Using Exponential Extra Production Rate for Summers and Strobel Neutrals

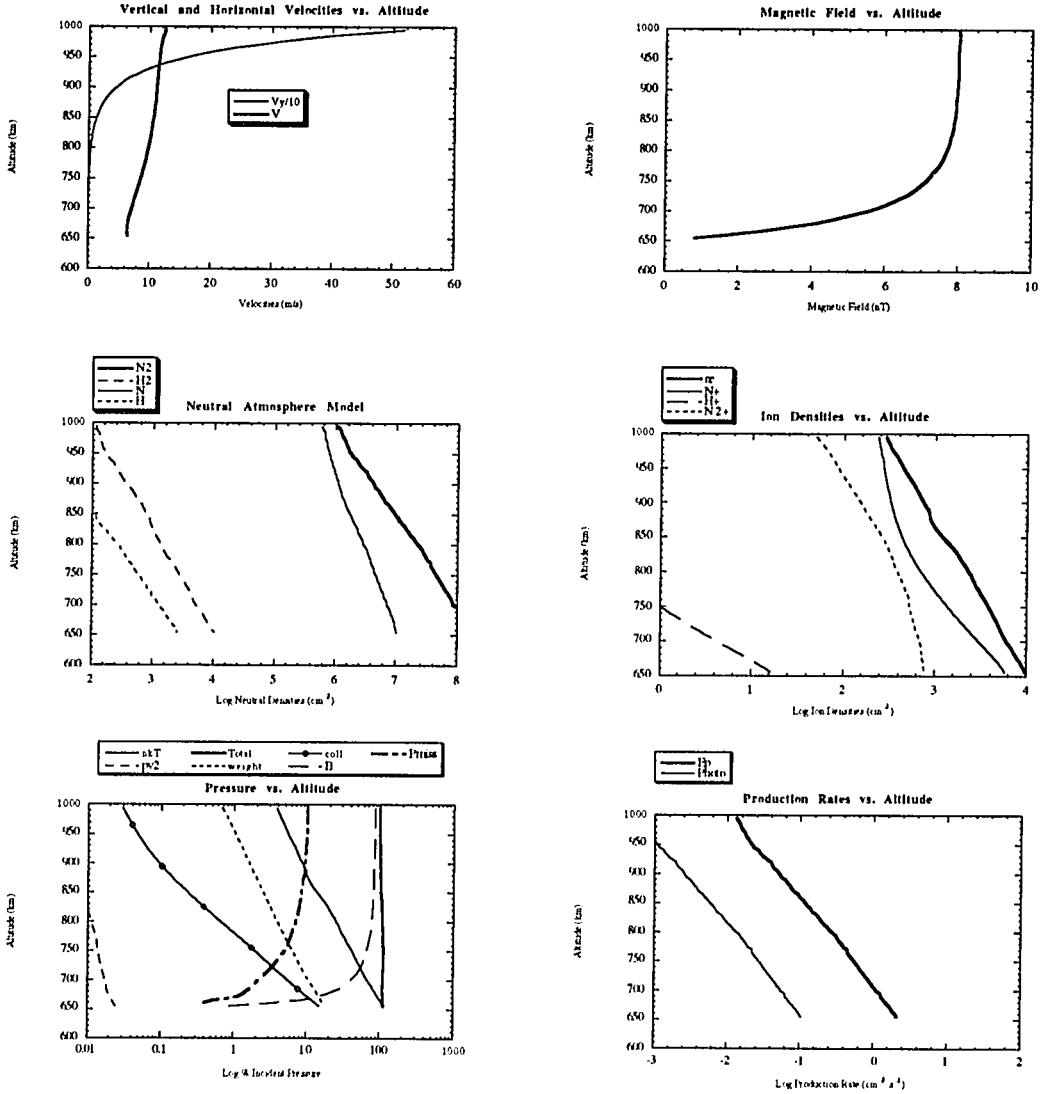


Figure 19. Flow/field results with *Summers and Strobel* [1991] neutrals when the extra production rate is assumed to follow the neutral density profile. Refer to Figure 18 for comments, however note here that the total ion density is less than the total electron density at altitudes around 850 km (see text for discussion).

## Results Using Exponential Extra Production Rate for Krasnopolsky et al. Neutrals

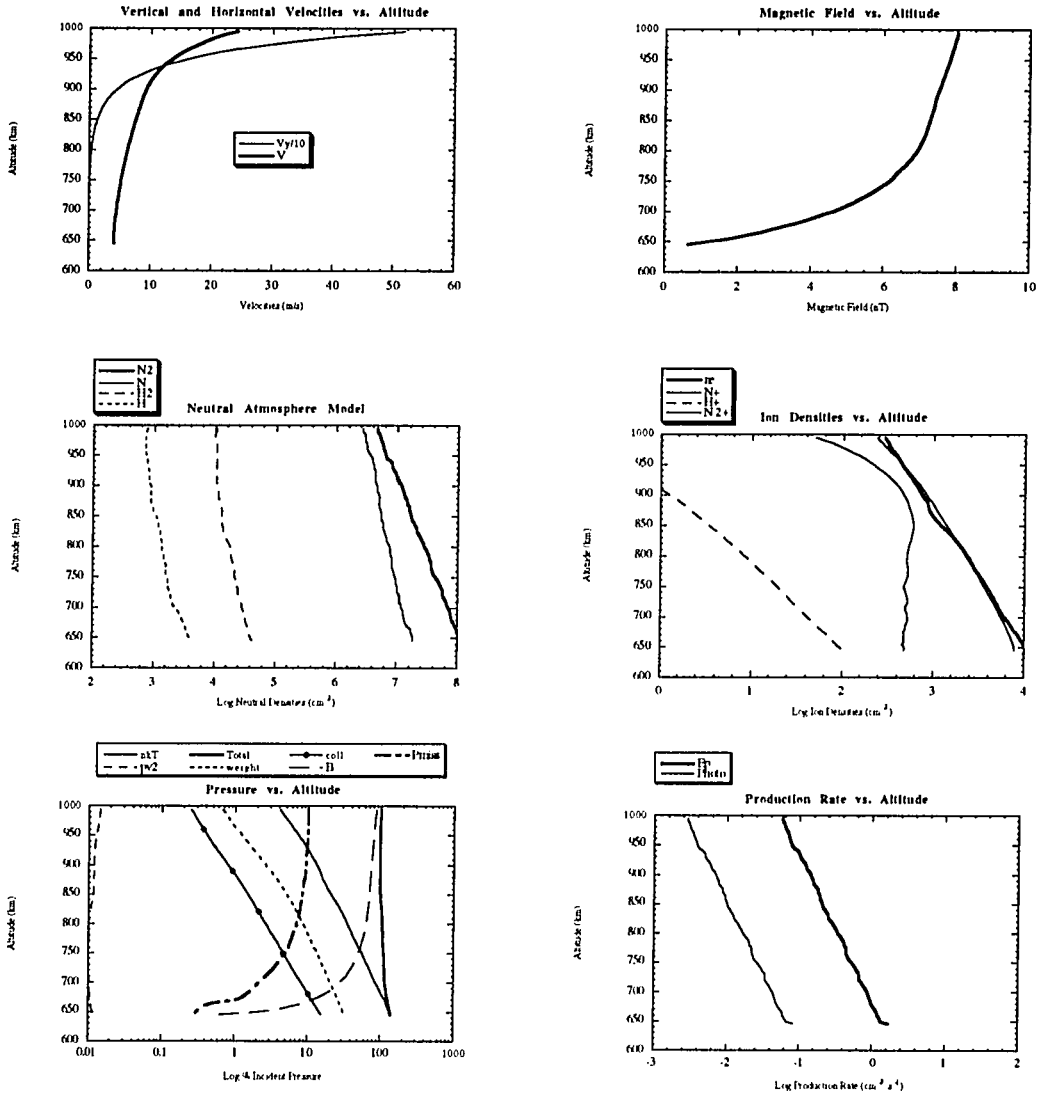


Figure 20. Flow/field results with *Krasnopolsky et al.* [1991] neutrals when the extra production rate is assumed to follow the neutral density profile. Refer to Figure 18 for comments, and note that, as in the Broadfoot et al. neutral run, the total ion density exceeds the total electron density at altitudes around 850 km (see text).

## VIII. Conclusions

The thrust of this study has been to analyze the unique plasma interaction between Triton and Neptune's magnetosphere. By incorporating the plasma dynamics learned from the Venus-solar wind interaction, this study sheds old light on a new problem. Previous models attempting to reproduce the experimental results from the Voyager 2 spacecraft have all failed to fully incorporate the magnetosphere-ionosphere interaction into their studies. This study demonstrates the importance of incorporating the flowing dynamics into the analysis of Triton's ionosphere with five fundamental conclusions.

The first conclusion is the simple realization that the topside ionosphere, i.e., altitudes greater than the peak electron density at 350 km, cannot be in photochemical equilibrium. Photochemical equilibrium requires the plasma scale height to equal twice the neutral scale height. According to *Tyler et al.* [1989], the plasma scale height for the topside ionosphere is 120 km. Assuming the dominant neutral species is molecular nitrogen, an incontestable assumption, it is easy to calculate the neutral scale height for this same altitude regime to be 95 km. However, this result also implies that the topside ionosphere is not convectively dominant; convective flow requires the neutral and plasma scale heights to be equal [*Cloutier et al.*, 1969]. Therefore we conclude that the interaction is subtle but necessary.

This is an important point, one which has either not been dealt with previously, or has been dealt with differently. In order to explain the scale height ordering

$$2H_n > H_i > H_n$$

other researchers such as *Yung and Lyons* [1990], and *Summers and Strobel* [1991] invoke a substantial ion loss off the top of the ionosphere, $3.4 \times 10^{25} \frac{1}{s}$ [*Summers and Strobel*, 1991]. This global ion escape effectively reduces the topside scale height thereby rectifying the discrepancy. This study proposes downward convective flow, intermediary between domination and nonexistence, explains the suppression of the topside plasma scale height. Furthermore, the realization that this interaction is in many ways similar to Venus, and that fifteen years of Venus study have not shown there to be a significant ion loss but, rather, extensively documents the suppression of the topside scale height due to downward convection [*Cloutier et al.*, 1987], strongly suggests that downward convection is a very real probability in Triton's ionosphere. Indeed, the final answer may be that both mechanisms contribute to the suppression of the topside plasma scale height. In any case, downward flow certainly cannot be ignored above altitudes of 650 km.

This downward flow is a result of the excess pressure the flowing magnetosphere represents to Triton's atmosphere. It has been explained that this excess pressure must get transferred to the neutrals. Furthermore, it has become apparent that due to the low gravitational attraction of the moon, and the relatively intense ionization of the ionosphere, the topside plasma does not come into hydrostatic equilibrium. The failure of the weight of the ionosphere, represented in figures 14-16 and figures 18-20, to match the thermal ionospheric pressure, indicates that the ionosphere is likely in diffusive equilibrium with the neutral atmosphere. This is our second conclusion.

The large electron and ion densities observed in Triton's ionosphere were reproduced in the flow/field model. From figures 14-16 and 18-20, it is apparent that photoionization is not able to sustain such high levels of ionization. Rather, another form of ionization is needed to produce Triton's ionosphere. The flow/field model is able to

provide some interesting information about this necessary extra production. First of all, figures 18-20 show that this ionization source is necessarily greater than photoionization by, roughly, a factor of ten to twenty. Furthermore, these figures show that this extra production follows the same scale height as photoionization. We know that photoionization is dependent only on the density of the neutrals in the optically thin regime, and thus the extra production term must also be chiefly dependent on the density of the neutrals. This hints that the process is likely collisional, the third conclusion.

According to studies of the Pioneer Venus data concerning the solar wind interaction with Venus' ionosphere, the downward flow shuts off just below the exobase [*Cloutier et al.*, 1987]. As mentioned before, this is entirely consistent with the theory which says that at the exobase collisions dominate over all other pressures and forces. The collisions act as a retarding force and stop the flow: a very intuitive result. However, a direct effect of the ions' vertical velocity going to zero is that the magnetic field magnitude must also go to zero at this same altitude. The collisions disengage the magnetic field from the plasma by breaking the frozen-in-flux condition. This all happens within a scale height of the exobase.

This study concludes that the vertical flow stops no lower than 650 km (see figures 14-16). As the flow terminates, the magnetic field disappears. Using the value for the neutral scale height calculated in equation (27), the exobase must occur near

$$r_{exo} = r_{stop} + H_e$$

$$r_{exo} \approx 650 \text{ km} + 100 \text{ km} = 750 \text{ km}$$

Therefore the fourth conclusion is that the exobase is near the altitude 750 km. This more closely agrees with the exobase designated by *Broadfoot et al.* [1989] than the recently calculated value of 870 km by *Krasnopolsky et al.* [1993].

Finally, this study allows one to say something interesting about the mysterious production process occurring in Triton's ionosphere. Recall that the resultant extra production term required for agreement with observed electron densities was approximately an order of magnitude higher than photoionization. This ionization process has been postulated to be impact ionization by hot magnetospheric electrons [*Tyler et al.*, 1989; *Strobel et al.*, 1990a]. The fact that this ionization rate follows the neutral scale height argues for this hypothesis, however, the process by which it occurs comes into question. Since the externally imposed magnetic field cannot exist at altitudes lower than 650 km, the previous mechanisms put forth in the literature are necessarily incorrect. For example, in the *Ip* [1990] paper he states, "Since the passage of the ionizing electrons depends on the tunneling effect of the draped magnetic field, an extra factor to be invoked is the existence of magnetic field down to an altitude of about 200 km. Otherwise, the present scenario of magnetospheric electron precipitation would not be valid."

The final conclusion is thus: the present scenario of magnetospheric electron precipitation is not valid. So what is the mechanism by which Triton's atmosphere becomes so highly ionized? This question remains unresolved, however a possible explanation still involves the magnetospheric electrons. This study concludes that the electrons cannot be bouncing along the magnetic field lines and curvature drifting into the ionosphere as *Hartle et al.* [1982] and *Ip* [1990] have postulated. But perhaps these hot electrons reach the lower ionosphere in a different way.

In work done by *Kramer et al.* [1992], it was shown that superthermal ions in the ionosphere of Venus progress down the atmosphere in a manner dominated by the magnetic field. However, once the magnetic field vanishes these superthermals are released and driven down the atmosphere where they quickly collide with the neutrals. Therefore we postulate the mechanism by which the ionosphere of Triton is ionized

involves impact ionizations from hot magnetospheric electrons colliding with neutrals, but flowing independently of the magnetic field. This is fundamentally different from previous models and is an area of continuing research.

This study shows that by examining the details of the plasma interaction between Triton and Neptune's corotational magnetosphere, the results from Voyager 2 instruments can be reproduced. Furthermore, the application of methods used at Venus and Mars reveal a different possible mechanism for the structure of the top-side ionosphere, namely downward convective flow. The inclusion of magnetic field effects in this study is unique; all previously published studies have assumed an unmagnetized Triton ionosphere. Finally, this study shows the necessity of an extra production rate in the ionosphere and points to the likelihood of magnetospheric precipitation as the cause. In the 1992 *Lyons et al.* paper, they postulated that, "Triton [may be] the first planetary body discovered in the solar system whose upper atmospheric chemistry is clearly controlled by a nonsolar source." This study supports this statement and concludes that since the incident magnetospheric plasma ionizes the majority of the ionosphere, the Triton-Neptune plasma interaction is the most dominant planetary body interaction discovered in the solar system.

## References

Belcher, J. W. et al., Plasma Observations near Neptune: Initial Results from Voyager 2, *Science*, 246, 1478-1483, 1989.

Brace, L. H., Taylor, H. A. Jr., Gombosi. T. I., Kliore, A. J., Knudsen, W. C., Nagy, A. F., The Ionosphere of Venus: Observations and their Interpretation, in Venus edited by Hunten, D. M, Colin, D. M., Donahue, T. M., Moroz, V. I., U. Arizona Press, Tucson, 779-840, 1983.

Broadfoot, A. L., et al., Ultraviolet Spectrometer Observations of Neptune and Triton, *Science*, 246, 1459-1466, 1989.

Cloutier, P. A. Solar Wind Interaction with Planetary Ionospheres, *NASA Spec. Publ., NASA Sp-397*, P-111, 1976.

Cloutier, P. A., Formation and Dynamics of Large-Scale Magnetic Structures in the Ionosphere of Venus, *J. Geophys. Res.*, 89, 2401, 1984.

Cloutier, P. A., Daniell, R. E. Ionospheric currents induced by solar wind interaction with planetary atmospheres, *Planet Sp. Sci.*, 21, 463, 1973.

Cloutier, P. A., and Daniell, R. E. Jr., An Electrodynamic Model of the Solar Wind Interaction with the Ionospheres of Mars and Venus, *Planet. Space Sci.*, 27, 1111, 1979.

Cloutier, P. A., Daniell Jr., R. E., Butler, D. M., Atmospheric Ion Wakes of Venus and Mars in the Solar Wind, *Planet Space Sci.*, 22, 967-990, 1974.

Cloutier, P. A., McElroy, and F. C. Michel, Modification of the Martian Ionosphere by the Solar Wind, *J. Geophys. Res.*, 74, 6215-6228, 1969.

Cloutier, P. A, Stewart, B. K., Taylor, H. A. Jr., Missing Pressure in the Dayside Ionosphere of Venus, *Geophys. Res. Let.*, 19, 1431-1434, 1992.

Cloutier, P. A., Tascione, T. F., Daniell Jr., R. E., An Electrodynamic Model of Electric Currents and Magnetic Fields in the Dayside Ionosphere of Venus, *Planet Space Sci.*, 29(6), 635-652, 1981.

Cloutier, P. A., Tascione, T. F., Daniell Jr., R. E., Taylor, H. A., Wolf, R. S., Physics of the Interaction of the Solar Wind with the Ionosphere of Venus: Flow/field models, in Venus edited by Hunten, D. M, Colin, D. M., Donahue, T. M., Moroz, V. I., U. Arizona Press, Tucson, 941-979, 1983.

Cloutier, P. A., Taylor, H. A., McGary, J. E., Steady State Flow/Field Model of Solar Wind Interaction With Venus: Global Implications of Local Effects, *J. Geophys. Res.*, 92(A7), 7289-7307, 1987.

Connerney, J. E. P., Acuña, M. H., Ness, N. F., The Magnetic Field of Neptune, *J. Geophys. Res.*, 96, 19023-19042, 1991.

Daniell, R. E. and Cloutier, P. A., Distribution of Ionospheric Currents Induced by the Solar Wind Interaction with Venus, *Planet Sp. Sci.*, 25, 621, 1977.

Dessler, A. J., Solar Wind and Interplanetary Magnetic Field, *Rev. Geophys.*, *5*, 1, 1967.

Fabian, A. C., Cooling Flows in Clusters and Galaxies, Dordrecht: Kluwer, 1988.

Hanson, W. B., Structure of the Ionosphere, in Satellite Environment Handbook, edited by F. S. Johnson, Stanford University Press, Palo Alto, Calif., 41, 1961.

Hartle, R. E., Sittler, E. C. Jr., Ogilvie, K. W., Scudder, J. D., Lazarus, A. J., Atreya, S. K., Titan's Ion Exosphere Observed from Voyager 1, *J. Geophys. Res.*, 87(A3), 1383-1394, 1982.

Hoogeveen, G. W., A Flow/Field Model of a Hot Magnetized Plasma Interacting with a Cold Neutral Atmosphere, Master's Thesis, Rice University, Houston, 1993.

Ip, W.-H., On the Ionosphere of Triton: An Evaluation of the Magnetospheric Electron Precipitation and Photoionization Effects, *Geophys. Res. Let.*, 17, 1713-1716, 1990.

Kirby, K., Constantinides, E. R., Babeu, S., Oppenheimer, M., and Victor, G. A., Photoionization and Photoabsorption Cross Sections of He, O, $N_2$, and $O_2$ for Aeronomic Calculations, *Atomic Data Nucl. Data Tables*, 23, 63-81, 1979.

Kramer, L., Cloutier, P. A., Taylor, H. A. Jr., Model of Superthermal Ions in the Venus Ionosphere, *J. Geophys. Res.*, 98, 3645-3658, 1993.

Krasnopolsky, V. A., Sandel, B. R., Herbert, F., and Vervack, R. J. Jr., Temperature, $N_2$, and N Density Profiles of Triton's Atmosphere: Observations and Model, *J. Geophys. Res.*, E2, 3065-3078, 1993.

Krishnakumar, E., and Srivastava, S. K., Cross Sections for the Production of $N_2^+$, $N^+ + N_2^{2+}$ and $N^{2+}$ by Electron Impact on $N_2$, *J. Phys. B: At. Mol. Opt Phys.*, 23, 1893-1903, 1990.

Krymskii, A. M., and Breus, T. K., Magnetic Fields in the Venus Ionosphere: General Features, *J. Geophys. Res.*, 93, 8459, 1988.

Landau, L. D., and Lifshitz, E. M., Fluid Mechanics, Addison-Wesley, Reading Mass., 314-317, 1966.

Luhmann, J. G., Russell, C.T., Elphic, R.C., Time Scales for the Decay of Induced Large-Scale Magnetic Fields in the Venus Ionosphere, *J. Geophys. Res.* 89(A1), 362-368, 1984.

Lyons, J. R., Yung, Y. L., Allen, M., Solar Control of the Upper Atmosphere of Triton, *Science*, 256, 204-206, 1992.

Majeed, T., McConnell, J. C., Strobel, D. F., Summers, M. E., The Ionosphere of Triton, *Geophys. Res. Let.*, 17, 1721-1724, 1990.

Mauk, B. H., Krimigis, S. M., Cheng, A. F., and Selesnick, R. S., Energetic Particles and Hot Plasmas of Neptune, To appear in: Neptune and Triton, University of Arizona Press, 1994.

Michel, F. C., Solar Wind Interaction with Planetary Atmospheres, *Rev. Geophys. Sp. Phys.* 9(2), 427-435, 1971.

Monnom, G., Eliot, M., Guidini, J., and Valckx, F. P. G., Physique Atomique, *C. R. Acad. Sc. Paris Serie B*, 425-428, 1975.

Morioka, Y., Aoyama, S., Kageyama, Y., Hayaishi, T., Suzuki, I. H., Isoyama, G., Asaoda, S., Ishiguro, E., and Nakamura, M., Dissociative Photoionization of $N_2$ from Threshold to 29 eV, *J. Phys. B At. Mol. Phys.*, 17, 2795-2802, 1984.

Ness, N. F., Acuña, M. H., Burlaga, L. F., Connerney, J. E. P., Lepping, R. P., and Neubauer, F. M., Magnetic Fields at Neptune, *Science*, 246, 1473-1477, 1989.

Neubauer, F. M., and Luttgen, A., On the Lack of a Magnetic Signature of Triton's Magnetospheric Interaction on the Voyager 2 Flyby Trajectory, *J. Geophys. Res.*, 96, 19171-19175, 1991.

Neubauer, F. M., Satellite Plasma Interactions, *Adv. Sp. Res.*, 10, 25-38, 1990.

Parks, G. K., Physics of Space Plasmas: An Introduction, Addison-Wesley Publishing Company, Redwood City, CA, 1991.

Phillips, J. L., Luhmann, J. G., Russell, C.T., Dependence of Venus Ionopause Altitude and Ionospheric Magnetic Field on Solar Wind Dynamic Pressure, *Adv. Sp. Res.* (GB), 5, 173-176, 1985.

Prasad, S. S., and Huntress, W.T. Jr., A Model for Gas Phase Chemistry in Interstellar Clouds: I. The Basic Model, Library of Chemical Reactions, and Chemistry among C, N, and O Compounds, *Astrophys. J. Suppl.*, 43, 1-35, 1980.

Russell, C. T., Elphic, R. C., Slavin, J. A., Initial Pioneer Venus Magnetic Field Results: Dayside Observations, *Science*, 203, 745-748, 1979.

Sauer, K., Baumgartel, K., Roatsch, T., McKenzie, J. F., A New Type of Plasma Flow Boundary: Relevance to the Planetopause at Mars, submitted to *J. Geophys. Res.*, 1991.

Spreiter, J. R., Summers, A. L., Rizzi, A. W., Solar Wind Flow Past Nonmagnetic Planets-Venus and Mars. *Planet Space Sci.* 18, 1281-1299, 1970.

Stevens, M. H., Strobel, D.F., Summers, M. E., Yelle, R. V., On the Thermal Structure of Triton's Thermosphere, *Geophys. Res. Let.*, 19, 669-672, 1992.

Stewart, B. K., A Modified Flow/Field Model of the Solar Wind Interaction with Mars, Ph.D. Thesis, Rice University, Houston, 1991.

Strobel, D. F., Cheng, A. F., Summers, M. E., Strickland, D. J., Magnetospheric Interaction with Triton's Ionosphere, *Geophys. Res. Let.*, 17, 1661-1664, 1990a.

Strobel, D. F., Summers, M. E., Herbert, F., Sandel, B.R., The Photochemistry of Methane in the Atmosphere of Triton, *Geophys. Res. Let.*, 17, 1729-1732, 1990b.

Summers, M. E., Strobel, D. F., Triton's Atmosphere: A Source of N and H for Neptune's Magnetosphere, *Geophys. Res. Let.*, 18, 2309-2312, 1991.

Tyler, G. L., Eshleman, V. R., et al., Radio Science Investigations of the Saturn System with Voyager 1: Preliminary Results, *Science*, 212, 201-206, 1981.

Tyler, G. L. et al., Voyager Radio Science Observation of Neptune and Triton, *Science*, 246, 1466-1473, 1989.

Wallis, M. K., Weakly-Shocked Flows of the Solar Wind Plasma through Atmospheres of Comets and Planets, *Planet. Space Sci.*, 21, 1647-1660, 1973.

Wu, C. Y. R., Lee, L. C., and Judge, D. L., Fluorescence from Photofragments as an Aid in Identifying New Molecular States: The $N_2$ Case, *J. Chem. Phys.*, 80, 4682,4685, 1984.

Yung, Y. L., and Lyons, J. R., Triton: Topside Ionosphere and Nitrogen Escape, *Geophys. Res. Let.*, 17, 1717-1720, 1990.